Fig. 1. Plaque morphology of TBEV Oshima clones. Oshima-A4, A9 and B11 exhibited small plaques, while Oshima-Cl showed large plaques. Oshima-A11, E2, E3, E7 and Oshima-pt showed a mixture of small and large plaques.

Fig. 2. Weight changes in mice following subcutaneous inoculations with TBEV Oshima clones. Five mice in each group were subcutaneously inoculated with TBEV Oshima clones and observed for 21 days. Mouse weight was observed daily and compared with that at day 0. Each mouse is represented by a line that connects the open or closed diamond-shaped boxes. Each box represents the observed ratio of weight change at observation day. The lines with the open and closed boxes indicate a living mouse and a mouse that eventually died during the observation period, respectively.

Fig. 3. Viral load in brains and spleens. Three mice per group were subcutaneously infected with 10^4 PFU of TBEV Oshima clones, and their brains and spleens were collected at day 9 p.i.. (A) Infectious viral load in the brain. (B) Copy numbers of TBEV genome in the spleen. Oshima-pt, A11, C1, E2, E3 and E7, which showed a weight reduction in the infected mice, are indicated by closed diamond boxes. Oshima-A4, A9 and B11, which showed no weight reduction in the infected mice, are indicated by open diamond boxes. Error bar: SD, P: ANOVA.

Fig. 4. Position of the amino acid substitution Glu_{122}→Gly in E protein. The amino acid at position 122 of E protein is glutamic acid (E), and it is located at domain II of E protein. (A). Dimer structure of E protein of TBEV Oshima 5-10 strain. (B). Trimer structure of E protein of TBEV Oshima 5-10 strain. Arrows point to the area of amino acid substitution from Glu_{122}→Gly.

Fig. 1

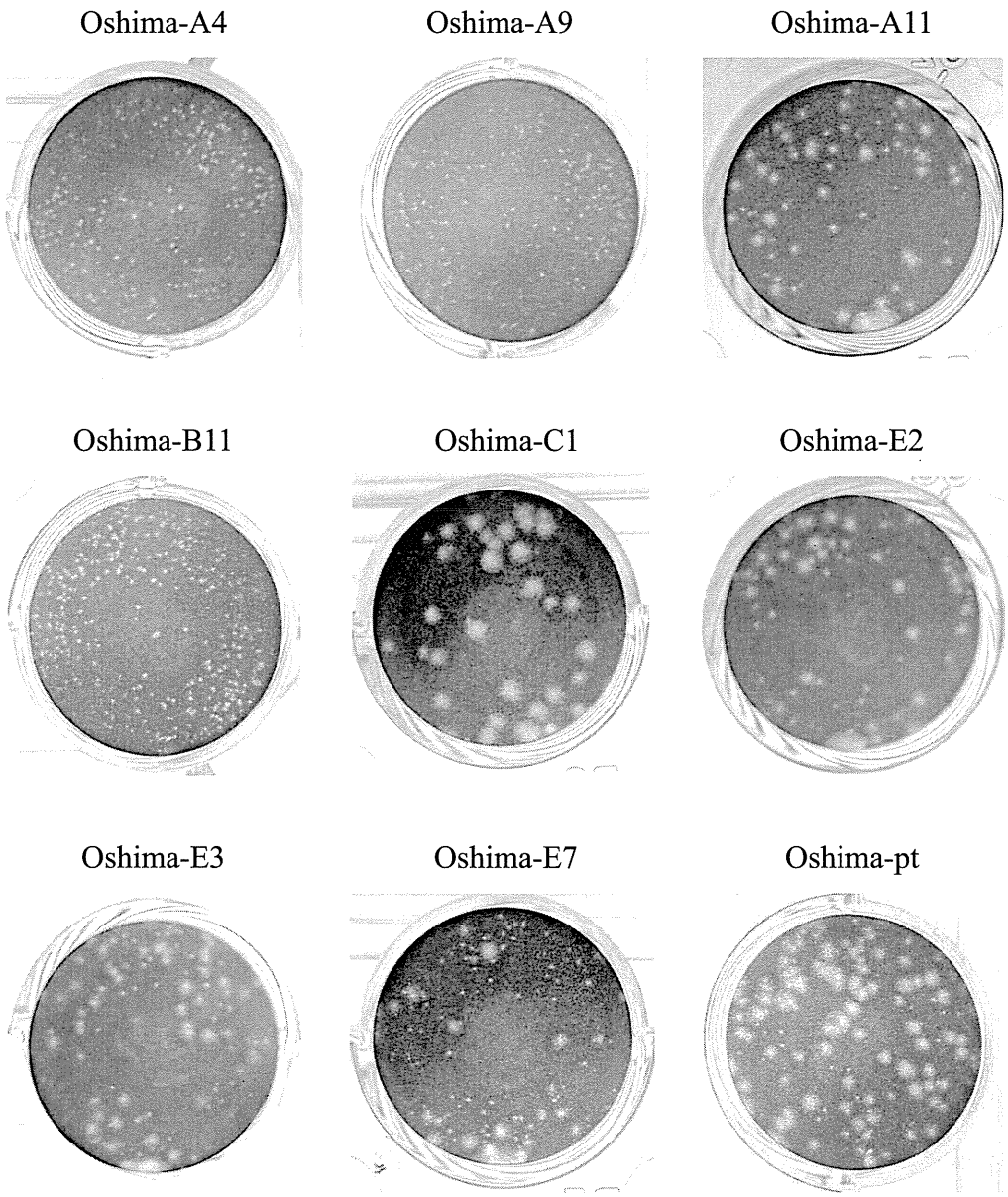
Oshima-A4
Oshima-A9
Oshima-A11
Oshima-B11
Oshima-C1
Oshima-E2
Oshima-E3
Oshima-E7
Oshima-pt

Fig. 2

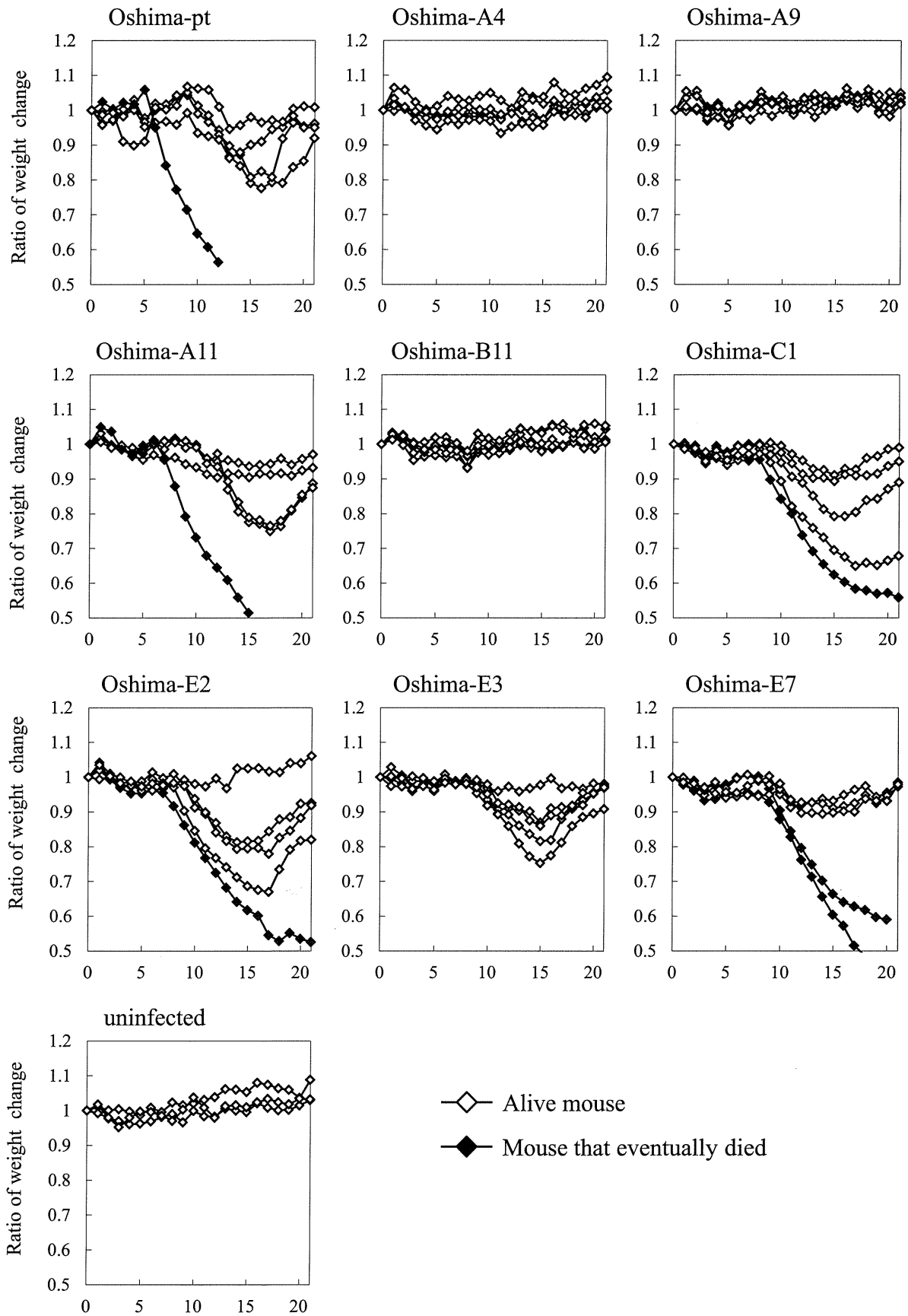
Oshima-pt
Oshima-A4
Oshima-A9
Oshima-A11
Oshima-B11
Oshima-C1
Oshima-E2
Oshima-E3
Oshima-E7
uninfected
Ratio of weight change
1.2
1.1
1
0.9
0.8
0.7
0.6
0.5
0
5
10
15
20
Alive mouse
Mouse that eventually died

Fig. 3

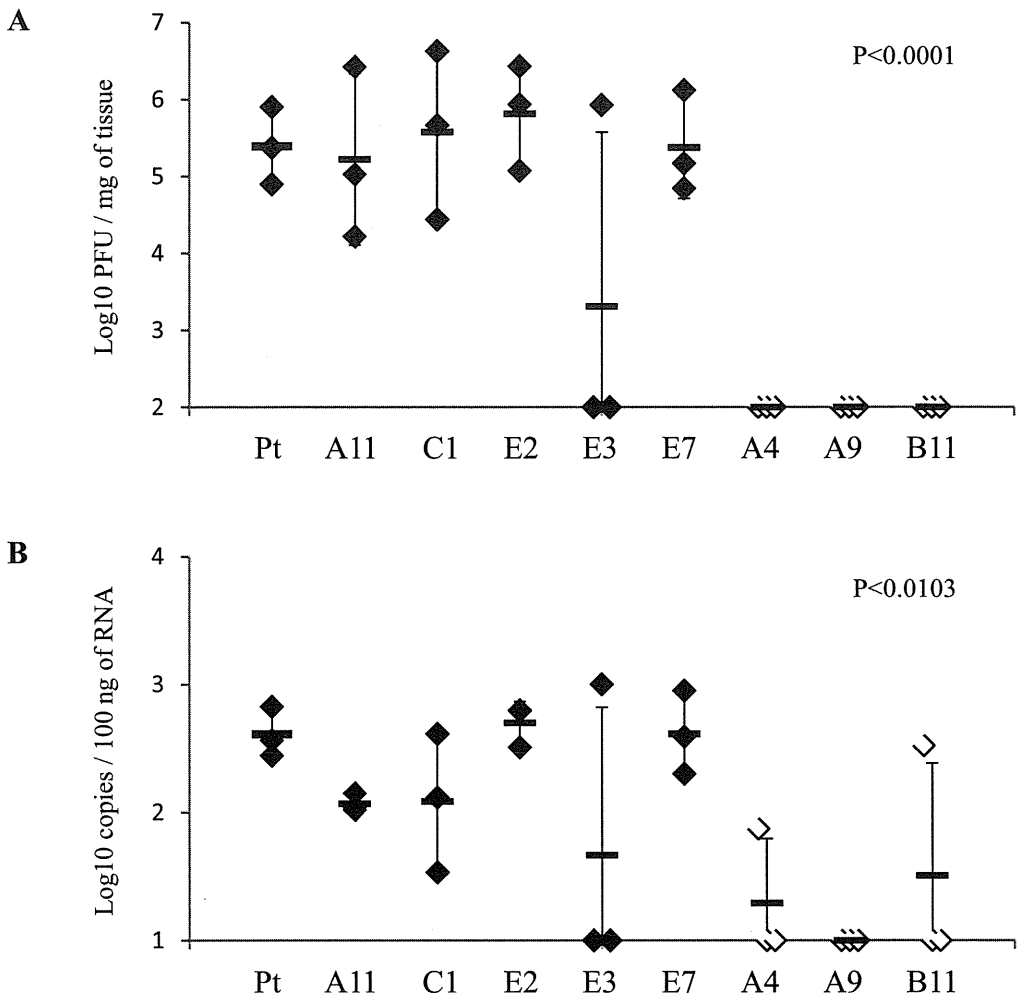
A
Log10 PFU / mg of tissue
7
6
5
4
3
2
P<0.0001
Pt
A11
C1
E2
E3
E7
A4
A9
B11
B
Log10 copies / 100 ng of RNA
4
3
2
1
P<0.0103
Pt
A11
C1
E2
E3
E7
A4
A9
B11

Fig. 4

A

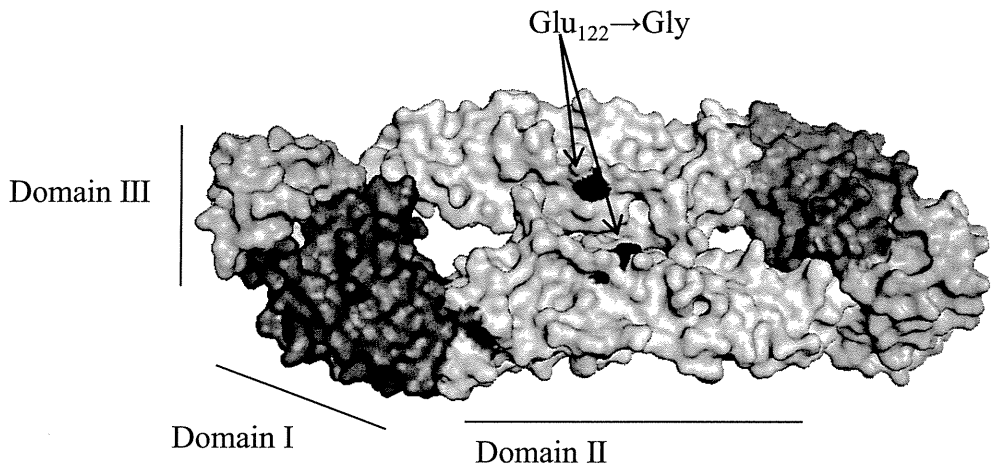
Glu122→Gly
Domain III
Domain I
Domain II

B

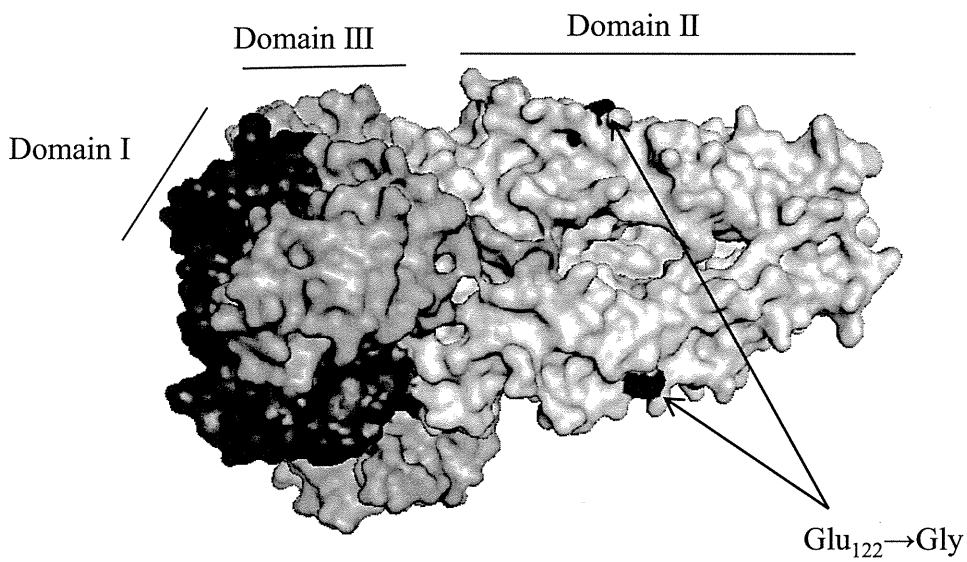
Domain III
Domain II
Domain I
Glu122→Gly

Journal of Virological Methods 193 (2013) 42–49

Contents lists available at SciVerse ScienceDirect

Journal of Virological Methods

journal homepage: www.elsevier.com/locate/jviromet

Rapid, whole blood diagnostic test for detecting anti-hantavirus antibody in rats

Takako Amada[a], Kumiko Yoshimatsu[a], Shumpei P. Yasuda[a], Kenta Shimizu[a], Takaaki Koma[a], Nobuhito Hayashimoto[b], Chandika D. Gamage[a], Sanae Nishio[a], Akira Takakura[b], Jiro Arikawa[a,*]

[a] Department of Microbiology, Graduate School of Medicine, Hokkaido University, Kita-ku, Kita-15, Nishi-7, Sapporo 060-8638, Japan
[b] Central Institute for Experimental Animals, 1430 Nogawa, Miyamae, Kawasaki 216-0001, Japan

Article history:
Received 1 November 2012
Received in revised form 18 April 2013
Accepted 29 April 2013
Available online 15 May 2013

Keywords:
ICG test
Seoul virus
IgG
HFRS
Hemorrhagic fever with renal syndrome
Laboratory animals

A B S T R A C T

Hantavirus is a causative agent of rodent-borne viral zoonoses, hemorrhagic fever with renal syndrome (HFRS) and hantavirus pulmonary syndrome. Seoul virus (SEOV) is a causative agent of urban and laboratory rat-associated HFRS worldwide. Surveillance of rodents has been done mainly by serological detection of hantavirus-specific antibodies by enzyme linked immunosorbent assay (ELISA) and immunofluorescent antibody assay (IFA). An immunochromatographic (ICG) test was developed with the N-terminal 103 amino acids of nucleocapsid protein of Hantaan virus expressed by *Escherichia coli* as an antigen to detect IgG antibody specific to hantavirus in sera from *Rattus* sp. animals. Antibody-detecting sensitivity of the ICG test was the same as that of ELISA and about 100-times higher than that of IFA. Overall sensitivities and specificities of the ICG test in comparison to ELISA and IFA for sera from 192 urban rats and 123 laboratory rats were 99.3% and 100%, respectively. Diluted whole blood samples without separation could be used for the ICG test. The ICG test enabled detection of antibodies to SEOV, Hantaan, Dobrava/Belgrade, and Thailand viruses, which are causative agents of HFRS throughout Eurasia. The ICG test is a rapid, simple and safe method for diagnosis of SEOV infection in rats.

1. Introduction

Hantaviruses belong to the genus *Hantavirus* of the family *Bunyaviridae*. Viruses in the genus *Hantavirus* contain causative agents of two important rodent-borne febrile zoonoses, hemorrhagic fever with renal syndrome (HFRS) in the Old World and hantavirus pulmonary syndrome (HPS) in the New World (Schmaljohn and Hjelle, 1997). The total number of HFRS patients worldwide is about 60,000–150,000 annually (Song, 1999). More than 90% of HFRS cases occur in Asian countries. On the other hand, hundreds and probably thousands of HPS cases have been reported in North and South American countries, respectively (Schmaljohn and Hjelle, 1997).

Twenty-three hantavirus species have so far been registered as members of the genus *Hantavirus*. Four of those virus species, Hantaan virus (HNTV), Seoul virus (SEOV), Dobrava/Belgrade virus (DOBV) and Puumala virus (PUUV), are known to be causative agents of HFRS, and Sin Nombre virus, Andes virus and other related viruses are known to be causative agents of HPS. Each of the hantaviruses has its own predominant reservoir animals as natural reservoirs, probably due to the consequence of co-evolution between reservoir animals and hantaviruses (Plyusnin et al., 1996). The HFRS- and HPS-causative hantaviruses so far detected all utilize rodents as reservoir animals. Therefore, endemic areas of HFRS and HPS have been confined to areas inhabited by specific reservoir rodents (Plyusnin and Morzunov, 2001). The only exception is an SEOV carried by the brown rat (*Rattus norvegicus*). SEOV has been found across a worldwide geographic range, from Asia to Africa, Europe, and both Americas (Childs et al., 1987; Cueto et al., 2008; Heyman et al., 2004, 2009; Korch et al., 1989; Lledo et al., 2002; McCaughey et al., 1996; Plyusnin and Morzunov, 2001; Reynes et al., 2003; Seijo et al., 2003; Truong et al., 2009; Wang et al., 2000; Weissenbacher et al., 1996; Wu et al., 2007), probably due to the migration of rodent reservoirs through international transportation by ship. Laboratory rat-associated HFRS caused by SEOV infection has also been reported in institutions and universities in Asia and Europe (Lloyd et al., 1984; Zhang et al., 2010). Therefore, extensive serological surveillance of rats is important for prevention of both urban rat- and laboratory rat-associated HFRS infection. Surveillance of rodents has been done mainly by serological detection of hantavirus-specific antibodies using enzyme linked immunosorbent assay (ELISA) and immunofluorescent antibody assay (IFA). However, more rapid, simple and safe diagnostic methods are required for rodent surveys.

In this study, an immunochromatographic (ICG) strip test developed for detection of SEOV IgG antibody in blood from *Rattus* spp.

* Corresponding author. Tel.: +81 11 706 6905; fax: +81 11 706 6906.
E-mail addresses: j_arika@med.hokudai.ac.jp, yosimatu@med.hokudai.ac.jp (J. Arikawa).

0166-0934/$ – see front matter © 2013 Elsevier B.V. All rights reserved.
http://dx.doi.org/10.1016/j.jviromet.2013.04.021

2. Materials and methods

2.1. Viruses and bacteria

SEOV strain SR-11 (Kitamura et al., 1983), Thailand virus (THAIV) strain thai749 (Elwell et al., 1985), HTNV strain 76-118 (Lee et al., 1982) and Dobrava/Belgrade virus (DOBV) strain Saaremaa (Nemirov et al., 1999) were propagated in Vero E6 cells as described previously (Yasuda et al., 2012). Mouse hepatitis virus (MHV) strain Nu67 was propagated in DBT cells as described previously (Kunita et al., 2011). *Mycoplasma pulmonis* strain m53 was cultured as described previously (Atobe and Ogata, 1974). Culture supernatants were stored at −80 °C until use.

2.2. Experimental infection of laboratory rats with SEOV

Two six-week-old WKAH/hkm female rats (SLC, Hamamatsu, Japan) were inoculated intraperioneally with 6×10^4 FFU of SEOV (strain SR-11), THAIV (thai749) or DOBV (Saaremaa) as described previously (Yasuda et al., 2012). Serum specimens were collected from the tail vein of a rat at the time of inoculation (day 0) and at 3, 6, 9, 13, 16, 19, 23, 27, 34, 40 and 49 days post inoculation (dpi) of SEOV. From rats inoculated with strain thai749 or Saaremaa, serum specimens were collected only at 49 dpi. Serum specimens obtained at 49 dpi were used as positive control serum specimen to evaluate the ICG strip test. Animal experimentation was performed after obtaining permission from the Institutional Animal Care and Use Committee of Hokkaido University. Experiments involving virus infection were performed in a BSL-3 facility. To examine the applicability of diluted whole blood specimens to the ICG system, blood samples were collected from the tail vein by the same procedure as that described above. Four microliters of blood was mixed with 150 μl of PBS to make a 1:75 dilution. A total of 18 sera were collected from SEOV-inoculated rats as described above, and blood was collected at the time of inoculation (day 0–2 samples) and at day 4 (2 samples), day 7 (2 samples), day 11 (2 samples), day 14 (2 samples), and day 49 (8 samples) post inoculation of SEOV.

2.3. Laboratory rat sera

A total of 110 laboratory rat sera were obtained from rats kept at SEOV prevalence-negative facilities and used as negative control sera. These sera were used for evaluation of ICG test specificity. The sera were screened initially for detecting antibodies to hemagglutinating virus of Japan (HVJ), sialodacryoadenitis virus (SDAV), *M. pulmonis*, Tizzer and HFRS by using a commercial IgG ELISA kit (MONILISA ®IV_A, MONILISA ®HANTA, Wakamoto Pharmaceutical, Tokyo, Japan). Positive samples against MONILISA ®HANTA were confirmed by IFA and Western blotting as described below. As shown in Table 3, the sera were divided into 4 groups depending on the conditions as follows. The first group consisted of 30 rat sera. These sera were negative by MONILISA ®IV_A, MONILISA®HANTA and IFA HANTA and were referred to as "Commercial IgG ELISA (−)". They were obtained from male and female rats aged between 10 and 48 weeks. The strains of rats were Wistar Hannover GALAS (BrlHan:WIST@Jcl), Fischer 344 (F344/N), Goto-Kakizaki (GK/Jcl) and Spontaneously Diabetic Torii (SDT/Jcl). The second group consisted of 40 sera that showed ELISA OD values greater than cut-off OD values (>0.2–2.1) to *Hantavirus* in MONILISA-HANTA but were finally confirmed as negative by IFA and WB. The third and forth groups consisted of IgG antibody positive to sialodacryoadenitis virus (SDAV) (20 sera) or *M. pulmonis* (20 sera, by the commercial ELISA test). As shown in Table 4, a total of 13 laboratory rat sera were obtained from rats kept at two facilities (facility A and facility B) where SEOV infection existed. Among the 13 sera, three sera were confirmed to be SEOV antibody-positive by IFA, IgG ELISA and IgM Western blotting, while the other 10 sera were confirmed to be antibody-negative.

2.4. Urban rat sera

A total of 192 serum specimens were obtained from *R. norvegicus* rat that were captured in urban areas in Hanoi and Haiphong port in Vietnam from 2009 to 2011(Koma et al., 2012). Among them, 26 were antibody-positive to *Leptospira interrogans* (Koma et al., 2012) and 21 were antibody-positive to hepatitis E virus (HEV) (Li et al., 2011).

2.5. Preparation of a recombinant antigen for hantavirus diagnosis

Since about 100 amino acids of the N-terminal region of the N protein of HTNV, SEOV, THIV, DOBV and Saaremaa viruses are highly conserved (Elgh et al., 1996; Yamada et al., 1995; Yoshimatsu et al., 1993), the HTNV-N terminal end was used as a representative antigen in this study. First, the coding region of the N-terminal 103 amino acids of the N protein of HTNV was amplified using primers (EIHNPATG, ccgGAATTCatggcaactatggaggaatt; HANSNP103-XhoI, tttaaCTCGAGcacattaccataac). A stop codon of the pET43.1b vector was used to terminate recombinant protein translation. Fragments were cloned into the EcoRI/XhoI restriction site of the pET43.1b vector (Merck KGaA, Darmstadt, Germany) in-frame with the NUS protein, and the resultant plasmids were introduced into *Escherichia coli* host BL21 (DE3). Expressed truncated NUS-tagged recombinant N protein of HTNV was purified using HisTrap HP columns (GE Healthcare, Little Chalfont, UK) according to the manufacturer's instructions. Since this region is closely related to HTNV and SEOV, the truncated antigen is termed HS103 in this manuscript. HS103 was used as ICG and ELISA antigens without deletion of the NUS-tag protein to maintain its solubility. Finally, the HS103 antigen possessed an NUS-tag and a histidine-tag in its N terminal region and another histidine-tag in its C terminal region. Recombinant N protein of HTNV was expressed in High five cells by a baculovirus vector (Schmaljohn et al., 1990) and used as an antigen for Western blotting.

2.6. Reference serological diagnosis methods

All samples in this study were first examined for anti-hantavirus antibodies either by commercial IgG ELISA and/or in-house ELISA followed by IgG IFA and IgM Western blotting. Serum specimens positive by commercial IgG ELISA and/or in-house IgG ELISA and IgG IFA were regarded as antibody-positive.

2.6.1. IgG IFA

IFA was carried out by methods described previously (Kunita et al., 2011; Morii et al., 1998; Yoshimatsu et al., 1993). MHV-Nu67-infected DBT cells were used for detection of antibodies against sialodacryoadenitis virus (SDAV). For detection of antibodies against *M. pulmonis*, *M. pulmonis* m53-infected BHK cells were used. For detection of antibodies against SEOV, SEOV-infected Vero E6 cells were used. The cells were spotted onto 24-well Teflon-printed slides, air-dried, fixed in acetone at 4 °C for 15 min, and then air-dried after rinsing with DW. The IFA antigens were stored at −20 °C until use. Fluorescein isothiocyanate-conjugated anti-rat immunoglobulin (heavy and light chains) goat IgG (Cappel Laboratories, Cochranville, PA) was used as the second antibody. IFA titers were expressed as the reciprocal of the highest serum dilution that caused characteristic fluorescence in cells. Serum specimens were examined after 1:100 dilution.

2.6.2. IgG detection by in-house ELISA

Ninety-six-well plates were first coated with 1 μg/ml of HS103 in PBS for 1 h at 37 °C as a capture antigen. After being washed three times with PBS containing 0.05% Tween 20 (PBS-T), the plates were blocked with PBS containing 3% bovine serum albumin (BSA) for 1 h at 37 °C. After blocking, rodent sera were diluted at 1:200 with ELISA buffer (PBS containing 0.5% BSA and 0.05% Tween 20) and added to the plates. After incubating for 1 h at 37 °C, the cells were washed three times with PBS-T. Bound antibody was detected with horseradish peroxidase (HRP)-labeled goat anti-rat IgG antibody (Invitrogen, Carlsbad, CA, USA) for 1 h at 37 °C. After being washed as above, color reactions were performed with o-phenylenediamine dihydrochloride (OPD) (Sigma–Aldrich, St. Louis, MO) and were allowed to develop for 10 min. Absorbance was measured at 450 nm by using a SpectraMax 340 microplate spectrophotometer (Molecular Device, Sunnyvale, CA). The optical density (OD) of each test sample was subtracted from the OD of the corresponding dilution of the unspecific antigen run on the same microtiter plate. Samples with titers of less than 0.2 were considered negative for IgG antibody.

2.6.3. IgM detection by Western blotting

Recombinant N protein of HTNV expressed by a baculovirus vector (Schmaljohn et al., 1990) was prepared in High five cells. The cell pellet was diluted to 300 μg/ml in sample buffer [1% sodium dodecyl sulfate (SDS), 1% β-mercaptoethanol, 0.05% bromophenol blue, and 10% glycerol] at 95 °C for 2 min. After incubation on ice, the cell lysate was subjected to polyacrylamide gel electrophoresis (PAGE) with precast gel (ePAGEL 10–20%, ATTO, Tokyo, Japan) and developed at 40 mA for 2 h. The developed proteins were then transferred to a polyvinylidene difluoride (PVDF; ATTO) membrane in transfer buffer (0.1 M Tris, 0.192 M glycine, and 5% methanol) at 2 mA/cm^2 for 60 min using a semi-dry system. The membrane was immersed in BlockAce (Dai Nippon Pharmaceutical, Osaka, Japan) for 1 h at room temperature and washed tree times with PBS. Rodent sera were diluted 1:200 in PBS and applied to the PVDF membrane by the use of Screener Blotter (Sanplastec Inc., Osaka, Japan). The membrane was then washed with PBS and immersed in a 1:5000 dilution of rabbit anti-rat IgM (BioFX Laboratories Inc.) at room temperature for 1 h. After washing, the membrane was immersed in a 1:500 dilution of HRP-labeled anti-rabbit IgG (BioFX Laboratories, USA) at room temperature for 1 h. Finally, the membrane was soaked in o-phenylenediamine dihydrochloride (OPD) (Sigma–Aldrich) at room temperature for 1 min (Koma et al., 2010) until an orange-brown color was visualized. Serum specimens that produced a clear color reaction were regarded as positive.

2.7. Avidity test

Avidity of the IgG antibody to hantavirus was assayed according to a procedure described previously (Gavrilovskaya et al., 1993; Kariwa et al., 1996). Serially diluted rat sera were added in duplicate to the wells of an ELISA plate coated with HS103 as in the in-house ELISA test. After incubation for 1 h at 37 °C, one set of serum dilution was washed three times with PBS-T containing 8 M urea and the other set of serum dilution was washed with PBS-T. Bound IgG was measured by addition of HRP-labeled anti-rat IgG (Invitrogen). The avidity value was calculated by the ratio of the ELISA OD value of an 8 M-urea-washed well to that of a well without urea treatment.

2.8. Preparation of an ICG strip

2.8.1. Preparation of colloidal gold conjugate

Gold colloid solution (WRGH2, Wine Red Chemical, Tokyo, Japan) was mixed with a two-times volume of 10 mM Tris–HCl (pH 8.15). Rabbit anti-rat IgG (Sigma–Aldrich) solution was diluted to 1 mg/ml with 10 mM Tris–HCl (pH 8.15). Equal volumes of the colloidal gold dilution and antibody solution were mixed in a siliconized tube. After brief sonication, the mixture was incubated for 20 min at room temperature. Then the mixture was centrifuged at 14,000 × *g* for 15 min. After removal of the supernatant, the pellet was resuspended with the original volume of blocking solution (0.05% polyethylene glycol 20,000 (PEG) and 2.5% casein sodium (Wako, Osaka, Japan) in 10 mM Tris–HCl (pH 9.2)). After incubating for 20 min at room temperature, the mixture was sonicated and centrifuged as described above. After removal of the supernatant, the same blocking procedure was repeated two more times. Finally, the pellet was sonicated and resuspended with phosphate-buffered saline (PBS) containing 5% trehalose and 1% BSA up to 12.5%.

2.8.2. Preparation of a conjugate pad

A glass-fiber conjugate pad (GFCP103000, Milipore, Billerica, MA, USA) was soaked in 0.5% casein in 20 mM PBS (pH 7.0) for 20 min. The pad was washed with 3.0% sucrose PBS and dried in air overnight. The colloidal gold conjugate prepared in (i) was put onto the pad at 200 μl/30 cm. The pad was dried in air overnight and kept at room temperature.

2.8.3. Preparation of an ICG test strip

The HS103 antigen prepared as described above and goat anti-rat IgG (KPL, Washington, DC, USA) were diluted with 12.5% casein sodium in 2.5 mM PBS (pH 7.0) to adjust the concentration to 1 mg/ml and then immobilized on a nitrocellulose membrane (Hi-Flow Plus 240 Membrane Card, 60 mm × 301 mm, Millipore) by drawing a thin line with a pen (Copic sketch Spare Nib, Too, Japan) at the test line and control line positions, respectively. After the membrane had been dried at room temperature for 15 min, the membrane was soaked in 20 mM PBS with 0.5% casein (pH 7.0) for 20 min to block the unsaturated area. Then the membrane was washed with 3.0% sucrose in DDW and dried overnight at room temperature. A sample pad (Whatman Chromatography Paper 3MM Chr, GE Healthcare), conjugate pad, nitrocellulose membrane and absorbent pad (Cellulose fiber sample pad CFSP203000, Millipore) were assembled on a Membrane Card. Finally, the combined membranes were cut into 3-mm-wide strips by using a paper cutter (PT62, Kokuyo, Osaka, Japan). The structure of the ICG strip is shown in Fig. 1A. The ICG strips were stored at room temperature in a dry and dark box until use.

2.8.4. Procedure of the ICG test

Serum dilution was prepared by mixing 2 μl of serum or 4 μl of blood with 150 μl of PBS in a microplate well, and an ICG strip was put directly into the well (Fig. 1B). After standing still for 15 min, the ICG line was examined by the naked eye. A serum sample that showed both test and control lines was regarded as positive, and a serum sample that showed only the control line was regarded as negative. Samples with the only test line were regarded as semi-positive.

3. Results

3.1. Determination of basic conditions of the ICG test

Various concentrations of labeled colloidal gold, HS103 antigen and goat anti-rat IgG antibody were tested with various combinations by using immune rat serum obtained at 49 days post infection with SEOV as a positive control. Consequently, 1 mg/ml of HS103 antigen and 1 mg/ml of goat anti-rat IgG antibody was used for the ICG strip as they showed the clearest test line and control line. Since

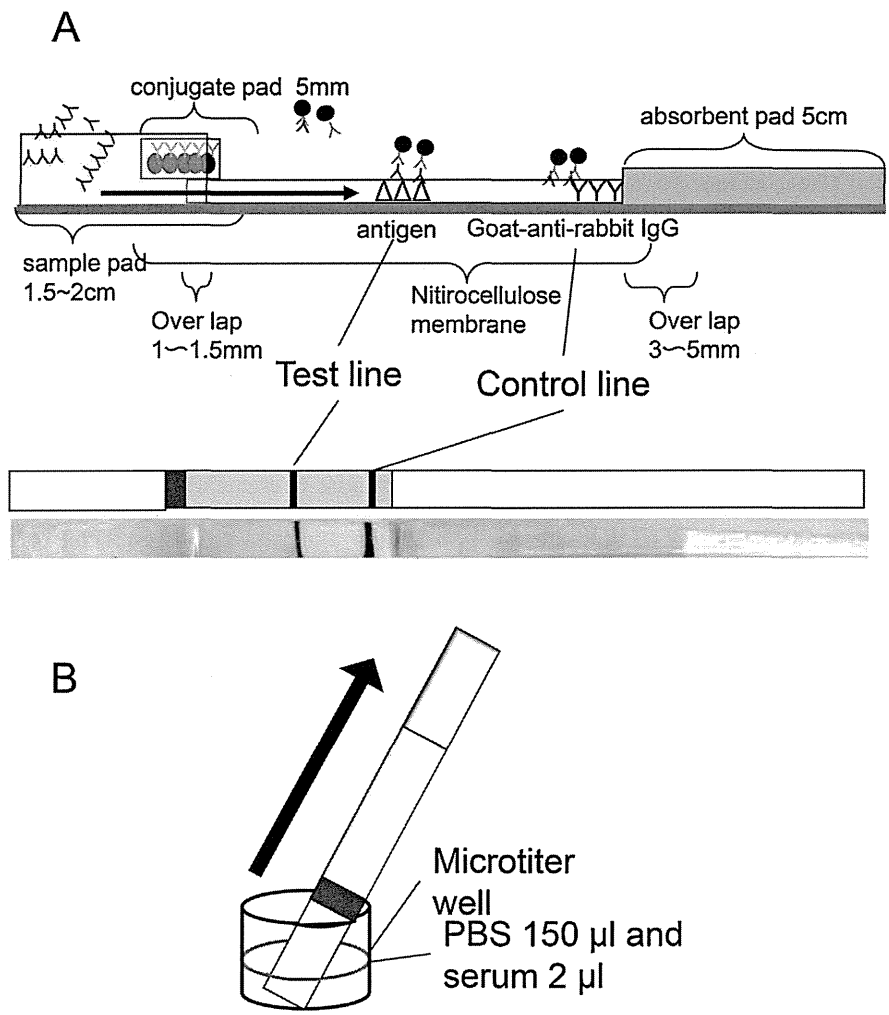

Fig. 1. Detection method and scheme of immunochromatographic test strip. (A) Structure of immunochromatographic test strip. HS103 antigen and goat anti-rabbit immune globulin were placed at the test line and control line, respectively. The ICG strip consisted of 4 membrane pads: sample pad, conjugate pad, nitrocellulose membrane and absorbent pad. (B) Detection method. Two microliters serum is diluted with 150 µl of PBS and then placed in a microtiter well. The strip is dipped in the solution. After incubation for 15 min, the test- and/or control line appeared.

the size of the absorbent pad determines the lateral flow speed and optimal sample volume, various volumes of samples were tested to determine the optimal sample volume. For the 3-mm-wide ICG strip, a sample volume of 150 µl gave the clearest results. Therefore, in the following experiment, serum dilution was prepared by mixing 2 µl of serum and 150 µl of PBS to make a final dilution of 1:75 and was applied to the ICG strip. The test needed 1–15 min for complete development at 4–30 °C. As shown in Fig. 2A, the ICG strip showed a clear test band against immune sera to THAIV, HTNV and DOBV with the same intensity as that with homologous HTNV immune sera.

3.2. Comparison of ICG test with ELISA and avidity in sera from rats inoculated experimentally

The results of ICG tests of serially collected rat sera were compared with ELISA OD and avidity % (Table 1). ELISA OD value and avidity titer increased with increase in the number of days past inoculation. The ICG test began to be positive on 6 dpi even though the ELISA OD value was very low (0.039) and the avidity value was 0%. With increase in the number of days post inoculation, ELISA OD value, avidity titer and intensity of test lines of the ICG test increased (data not shown) (Table 1).

3.3. Comparison of detection sensitivities of ICG test, ELISA and IFA in experimentally inoculated rat sera

Sensitivities for detection of SEOV antibody by the ICG test, ELISA and IFA were compared in sera from urban rats (Fig. 2B) and experimentally inoculated rats (Fig. 2C). As shown in the figures and Table 2, antibody detection limits of the ICG test were the same as those of ELISA and about 200-times higher than those of by IFA.

3.4. Comparison of the results of ICG tests and ELISA using laboratory rat sera

A total of 110 rat sera were obtained from laboratories where no hantavirus prevalence was confirmed (Table 3). As summarized in Table 3, sera from Group I (negative to hantavirus antibody by all diagnoses), Group II (high background ELISA OD by commercial ELISA but finally confirmed as negative by IFA) and Groups III and IV (antibody positive to SDAV and Mycoplasma) were all negative by the ICG test. A total of 9 sera from rats of more than 8 months old and 4 sera from retired rats (>12 months old) were obtained from facilities A and B where SEOV infection was confirmed. Three of the sera showed positive results by ELISA and the ICG test, and the other 6 sera were found to be negative by all methods. Sera

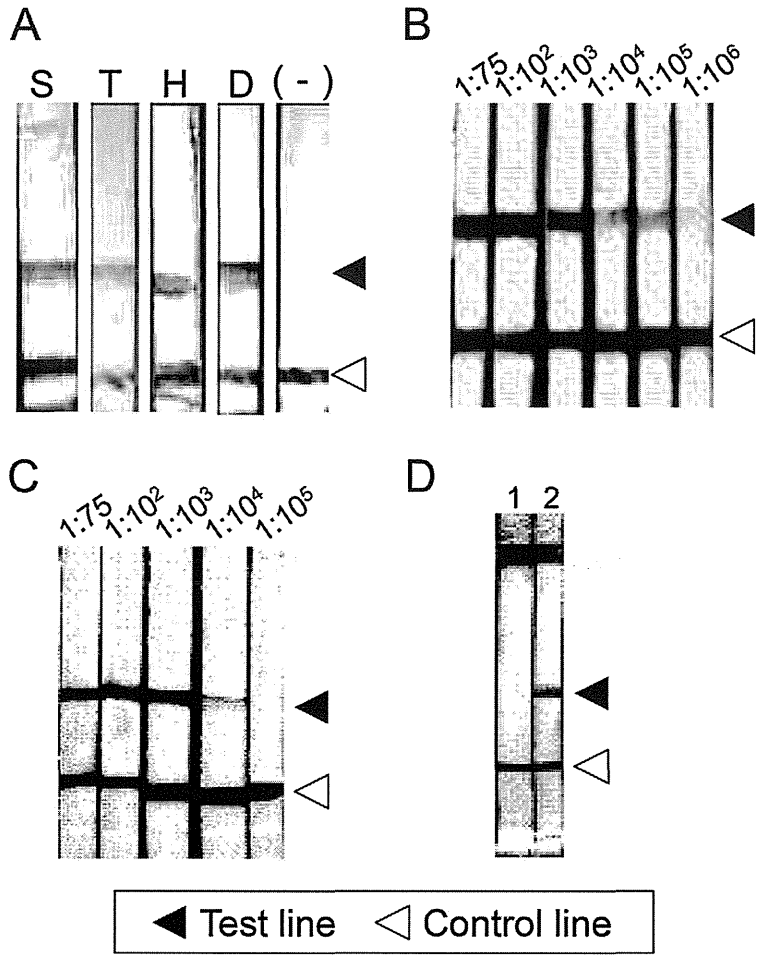

Fig. 2. (A) Cross-reactivity of the ICG test to antibodies against Murinae rodent-derived HFRS-related hantaviruses. Immune rat sera against 4 viruses. S: SEOV; T: THAIV; H: HNTV; D: DOBV; (−): uninfected. (B) ICG test lines in diluted sera. Serum from an urban rat obtained in Vietnam in 2011 (2011jan-wild-#20). (C) ICG test lines in diluted sera. Serum from an SEOV-inoculated laboratory rat (SEOV-Bday49:) on 49 dpi. Both were examined at 1:75 and 10-fold dilutions from 1×10^2. (D) ICG test strip after application of a whole blood sample. Blood from an uninfected rat was applied to strip 1 and blood from an infected urban rat was applied to strip 2.

from the 4 retired rats were also negative by commercial ELISA and in-house IgG ELISA and by IgM WB, but one of the sera showed positive results by the ICG test (Table 4).

3.5. Comparison of the results of ICG tests and the reference methods with urban rat sera

A total of 192 sera were obtained from Northern Vietnam, where SEOV infection is endemic (Table 5). A total of 35 sera that were IgG and IgM antibody-positive (26) and IgG antibody alone-positive (9) were also positive in the ICG test. On the other hand, negative sera and IgM alone-positive sera showed negative reaction in the ICG test. Therefore, it was confirmed that the ICG test is applicable for the detection of IgG antibody. A total of 153 sera from rats captured since January 2011 were examined for antibodies against HEV and *Leptospira*. Among them, 21 and 26 sera were found to be positive against HEV and *Leptospira*, respectively. These sera showed negative reaction in the ICG test. ICG reaction may not be affected by previously existing antibodies against other pathogens.

3.6. Evaluation of sensitivity and specificity of the ICG test using 315 rat sera

A total of 315 sera from laboratory rats and urban rats were examined for overall sensitivity and specificity (Table 6). The sensitivity of the ICG test was 38/38 (100%) and the specificity was 276/277 (99.3%). Efficacy ((sensitivity + specificity)/2) of the test was calculated to be 99.6%.

3.7. ICG test using diluted whole blood specimens

Diluted whole blood samples were used for ICG tests. A total of 4 μl of whole blood was mixed with 150 μl of PBS to obtain the same dilution as that of serum (1:75) and the mixture was applied directly to the ICG test. As shown in Fig. 2D, blood cells were trapped at the sample pad and clear bands were obtained either at the test line or control line. The intensities of the lines were the same as that with the serum specimen. Blood samples from uninfected laboratory rats and urban rats were all found to be negative by the ICG test. Blood samples collected periodically from inoculated experimentally rats were positive for the ICG specimens obtained early after inoculation (<4 days post inoculation). As shown in Table 7, sensitivity of the whole blood test was 16/16 (100%) and specificity was 44/44 (100%). These results indicated that the ICG test with whole blood was useful for the rapid diagnosis.

4. Discussion

The ICG test has been used widely for diagnoses of various infectious diseases by detecting an antigen or antibody against

Table 1
Comparison of ICG positivity and ELISA OD and avidity by using serially collected rat sera.

Days	Rat ID	IgG ELISA OD	IgG avidity assay	IgM	ICG
0	A	0.016	ND	–	–
	B	0.010	ND	–	–
3	A	−0.001	0%	–	–
	B	−0.001	0%	–	–
6	A	0.039	0%	+	+
	B	0.014	0%	–	–
9	A	0.122	0%	+	+
	B	0.037	0%	+	+
13	A	0.172	2.3%	+	+
	B	0.195	0%	+	+
16	A	0.234	6.4%	+	+
	B	0.430	2.8%	+	+
19	A	0.260	4.2%	+	+
	B	0.540	12.6%	+	+
23	A	0.389	13.6%	+	+
	B	0.581	38.4%	+	+
27	A	0.537	23.1%	+	+
	B	0.698	53.3%	–	+
34	A	0.544	12.6%	–	+
	B	0.912	38.4%	–	+
40	A	0.671	53.3%	–	+
	B	1.092	66.5%	–	+
49	A	0.984	57.0%	–	+
	B	1.069	55.8%	–	+

Table 2
Comparison of results obtained by ICG test, ELISA and IFA using experimentally or naturally infected rat sera with SEOV.

Groups	Serum ID	Highest dilution showing positive reaction		
		ICG	ELISA	IFA
Experimentaly inoculated rats	SEOV-A day0	–	–	–
	SEOV-A day6	$\times 10^3$	$\times 10^2$	$\times 10^2$
	SEOV-A day9	$\times 10^4$	$\times 10^3$	$\times 10^3$
	SEOV-A day13	$\times 10^5$	$\times 10^5$	$\times 10^3$
	SEOV-A day49	$\times 10^5$	$\times 10^5$	$\times 10^3$
	SEOV-B day0	–	–	–
	SEOV-B day6	–	–	–
	SEOV-B day9	$\times 10^2$	$\times 10^2$	$\times 10^2$
	SEOV-B day13	$\times 10^3$	$\times 10^2$	$\times 10^2$
	SEOV-B day49	$\times 10^4$	$\times 10^3$	$\times 10^3$
Urban rats	2011jan-wild-#3	$\times 10^5$	$\times 10^4$	$\times 10^3$
	2011jan-wil-#20	$\times 10^5$	$\times 10^4$	$\times 10^5$

–: <75.

Table 4
Results obtained by ICG tests and reference methods with sera of laboratory rats from an SEOV-prevalence facility.

Origin of rats	Total	ICG (+)/IgG (+), IgM (+)[a]	ICG (+)/IgG (−), IgM (−)[b]
Facility A	9	3/3	0/6
Facility B	4	NA[c]	1/4
Total	13	3/3	1/10

[a] No. of sera of ICG (+)/No. of sera of IgG ELISA (+) and IgM Western (+).
[b] No. of sera of ICG (+)/No. of sera of IgG ELISA (+) and IgM Western (−).
[c] NA, not available.

Table 5
Results of ICG tests of sera from urban rats in Vietnam.

Origin of rats	Total	ICG (+)/IgG (+), IgM (+)[a]	ICG (+)/IgG (+), IgM (−)[b]	ICG (+)/IgG (−), IgM (+)[c]	ICG (+)/IgG (−), IgM (−)[d]
August 2009	39	9/9	4/4	0/2	0/24
Jan 2011	100	10/10	4/4	0/2	0/84
July 2011	33	7/7	NA[e]	0/4	0/22
August 2011	20	NA	1/1	NA	0/19
Total	192	26/26	9/9	0/8	0/149

[a] No. of sera of ICG (+)/No. of sera of IgG ELISA (+) and IgM Western (+).
[b] No. of sera of ICG (+)/No. of sera of IgG ELISA (+) and IgM Western (−).
[c] No. of sera of ICG (+)/No. of sera of IgG ELISA (−) and IgM Western (+).
[d] No. of sera of ICG (+)/No. of sera of IgG ELISA (−) and IgM Western (−).
[e] NA, not available.

Table 6
Evaluation of the ICG test using 315 rat sera.

	ICG		Total
	Positive	Negative	
Reference method			
IgG positive[a]	38	0	38
IgG negative[b]	1	276	277
Total	39	276	315

Sensitivity of the ICG test was 38/38 (100%) and specificity was 276/277 (99.3%). Efficacy ((sensitivity + specificity)/2) was calculated to be 99.6%.
[a] No. of positive sera. Sera that were showed positive by both Moniliza®-Hanta (or IgG ELISA in-house) and IFA were regarded as positive.
[b] No. of negative sera. Sera that were negative either by Moniliza®-Hanta (or IgG ELISA in-house) or IFA were regarded as negative.

pathogens. In the field of hantavirus diagnosis, the first application of the ICG test for rapid serodiagnosis was Poc Puumala® (Hujakka et al., 2001a,b). Poc Puumala® was prepared for detecting a PUUV-specific IgM antibody in human sera. It was also applicable for detecting IgM antibody in sera of HPS patients infected with Andes virus (Navarrete et al., 2007). Diluted whole blood samples were also applicable to the ICG test, which has enabled rapid diagnosis at the bedside and in field surveys in vank voles, Norway lemmings (*Lemmus lemmus*) and sibling voles (*Microtus rossiaemeridionalis*) (Sirola et al., 2004).

Table 3
Results obtained by the ICG tests and reference methods with hantavirus-negative laboratory rat sera.

Group	Total	MONILISA®					IFA			ICG	
		Hantavirus	HVJ	SDAV	Myco	Tyzzer	Hantavirus	SDAV	Myco	+	–
I[a]	30	0	0	0	0	0	ND	ND	ND	0	30
II	40	40	0	0	0	0	0	ND	ND	0	40
III	20	0	0	20	0	0	ND	20	ND	0	20
IV	20	0	0	0	20	0	ND	ND	20	0	20
Total	110	40	0	20	20	0	0	20	20	0	110

These sera were collected in Central Institute for Experimental Animals (CIEA).
[a] Sera of group I were antibody-negative against any pathogen. Sera of group II showed higher ELISA OD in Monilisa®-Hanta, between 0.2 and 2.1, but they showed no reaction in IFA tests in hantavirus-infected cell antigen. Sera of group III and IV were antibody-positive against SDAV and *Mycoplasma*, respectively.

Table 7
ICG tests results with whole blood samples.

Origin of rats	Total	ICG(+)/IgG(+), IgM(+)	ICG(+)/IgG+, IgM−	ICG(+)/IgG−, IgM+	ICG(+)/IgG−, IgM−
Urban rat [a]	42	4/4	NA[b]	NA	0/38
Laboratory rats experimentally inoculated with SEOV[c]	18	11/11	1/1	NA	0/6
Total	60	15/15	1/1	NA	0/44

[a] Rats were captured in Vietnam in August 2011(18 samples) and February 2012 (24 samples). Among the February 2012 samples, were tested other etiological agents, 23 were antibody-positive to *Leptospira interrogans* and 21 were antibody-positive to hepatitis E virus (HEV)
[b] NA, not available.
[c] Blood were collected from rats on day 0 (2 samples), day 4 (2 samples), day 7 (2 samples), day 11 (2 samples), day 14 (2 samples), and day 49 (8 samples) post inoculation of SEOV. IgG antibody in blood by ICG test and in sera by reference methods were detected after 11 days inoculation.

However, Poc Puumala® is optimized for human IgM antibody detection in acute phase infection of PUUV. It showed lower sensitivity for detection of antibodies to Murinae rodent-derived hantaviruses such as HTNV, SEOV, and DOBV, which are major causes of HFRS in Eurasia. To solve this problem, a recombinant N protein of DOBV or HTNV was used for improvement of the ICG test as POC Dobrava-Hantaan® (Hujakka et al., 2003). However, both Poc Puumala® and POC Dobrava-Hantaan® are not an object for the rat IgG antibody detection in persistent phase. SEOV causes HFRS worldwide by transmission from urban and laboratory rats. Diagnosis in rat sera is also important from a public health point of view. Therefore, in this study, we have aimed to develop an effective ICG test for SEOV infection among *Rattus* species animals. In addition to SEOV, THAIV and related viruses were found from black rats of Indonesia (Plyusnina et al., 2004), Cambodia (Reynes et al., 2003), and Singapore (Johansson et al., 2010). Natural reassortant hantaviruses between HTNV and SEOV (Chen et al., 2012) and a HTNV outbreak among laboratory rats (Zhang et al., 2010) were reported from China. Therefore, attention must be paid to SEOV, THAIV, and HTNV as a rat-borne hantaviruses.

In previous studies, it was shown that an immunodominant and common antigenic site is located at the N-terminal end of the N protein of hantaviruses (Elgh et al., 1996; Yamada et al., 1995; Yoshimatsu et al., 1993). Therefore, in this study, the N-terminal 103 amino acids (HS103 antigen) was expressed by *E. coli* and used as an ICG antigen. At first, attempts were made to express the entire N protein of HTNV by using pRSET (data not shown) or PinPoint vectors in *E. coli* (Yoshimatsu et al., 1996). These trials recovered two problems. One was degradation of the recombinant N protein in *E. coli* and the other was poor solubility of the recombinant antigen. Truncation of the N protein gave better results for degradation, and fusion of the NUS-tag protein improved solubility of the recombinant antigen. As expected, the HS103 antigen was successfully applied to the ICG test for rat IgG detection. The ICG test enabled detection of the anti-SEOV IgG antibody in early-phase (6 dpi) serum from rats inoculated experimentally, which showed very low IgG ELISA ODs and IgG avidity value (0%). Furthermore, the sensitivity of the ICG test for detection of the anti-SEOV antibody was the same as that of ordinary ELISA and about 100-times higher than that of IFA. In addition to the high sensitivity, the ICG test showed no false-positive results in examination of many negative rat sera that were confirmed as being antibody-negative by multiple reference methods including commercial IgG ELISA, in-house IgG ELISA, IFA and IgM Western blotting.

The reason for the high sensitivity and specificity is not clear. However, the high sensitivity and specificity may have been due to the characteristics of HS103 antigen and colloidal gold particles. Truncation of the antigenic portion might increase its antigenicity and reduce non-specific binding. In addition to the selection of an antigen, selection of a system is important. Colloidal gold conjugation used in this study exceeded blue latex-conjugation (data not shown).

SEOV infection among laboratory rats is one of the most important zoonoses among laboratory animals. Therefore, serological monitoring of SEOV infection among laboratory rats has been carried out extensively. The ICG test presented here showed very high specificity even among sera that showed high background reactions by commercial IgG ELISA as well as antibody-positive sera to other infectious diseases. Furthermore, application of diluted whole blood in this ICG test enable rapid, safe and simple diagnoses with blood samples from tail veins of live animals. These results suggest that the ICG test will have future applications for diagnoses of laboratory rats.

The N-terminal end of the N protein is antigenically conserved among Murinae rodent-derived hantaviruses. Therefore, the ICG test with HS103 antigen enables detection of IgG antibodies in immune sera against HTN, SEOV, THAIV and DOBV. Epizootiological studies of rodents in East Asian countries have indicated the possibility of existing novel *Rattus*-derived hantaviruses. In addition to the cross-reactivity, high specificity of this ICG test even in wild rodents was demonstrated in this study. Therefore, an epizootiological study with our ICG test would be useful for finding novel hantaviruses from novel rodent reservoirs.

In conclusion, the ICG test has good analytical performance compared to the performance of reference methods and meets the requirements for a highly applicable field test.

Acknowledgements

This study was supported in part by the Program of Founding Research Centers for Emerging and Reemerging Infectious Diseases, MEXT, Japan. This work was also supported in part by a grant from the Global COE Program (Establishment of International Collaboration Center for Zoonosis Control) and also supported in part by Grants-in-Aid for Research on Emerging and Re-emerging Infectious Diseases from the Ministry of Health, Labour and Welfare including H22-emerging-ippan-006.

References

Atobe, H., Ogata, M., 1974. Pneumonitis in mice inoculated with *Mycoplasma pulmonis*: production of pulmonary lesions and persistence of organisms and antibodies. J. Vet. Med. Sci. 36, 496–503.
Chen, X.P., Yu, J., Li, M.H., Zhao, G.Y., Wang, W., Guo, W.P., Deng, X.Z., Zhang, Y., Fu, Z.F., Qin, X.C., Zhang, Y.Z., 2012. Pathogenicity of a natural reassortant hantavirus CGRn9415 in newborn rats and newborn mice. J. Gen. Virol. 93, 1017–1022.
Childs, J.E., Korch, G.W., Glass, G.E., LeDuc, J.W., Shah, K.V., 1987. Epizootiology of hantavirus infections in Baltimore: isolation of a virus from Norway rats, and characteristics of infected rat populations. Am. J. Epidemiol. 126, 55–68.
Cueto, G.R., Cavia, R., Bellomo, C., Padula, P.J., Suarez, O.V., 2008. Prevalence of hantavirus infection in wild *Rattus norvegicus* and *R. rattus* populations of Buenos Aires City, Argentina. Trop. Med. Int. Health 13, 46–51.
Elgh, F., Lundkvist, A., Alexeyev, O.A., Wadell, G., Juto, P., 1996. A major antigenic domain for the human humoral response to Puumala virus nucleocapsid protein is located at the amino-terminus. J. Virol. Methods 59, 161–172.
Elwell, M.R., Ward, G.S., Tingpalapong, M., LeDuc, J.W., 1985. Serologic evidence of Hantaan-like virus in rodents and man in Thailand. Southeast Asian J. Trop. Med. Public Health 16, 349–354.

Gavrilovskaya, I., Apekina, N., Okulova, N., Demina, V., Bernshtein, A., Myasnikov, Y., 1993. IgG avidity assay for estimation of the time after onset of hantavirus infection in colonized and wild bank voles. Arch. Virol. 132, 359–367.

Heyman, P., Baert, K., Plyusnina, A., Cochez, C., Lundkvist, A., Esbroeck, M.V., Goossens, E., Vandenvelde, C., Plyusnin, A., Stuyck, J., 2009. Serological and genetic evidence for the presence of Seoul hantavirus in *Rattus norvegicus* in Flanders, Belgium. Scand. J. Infect. Dis. 41, 51–56.

Heyman, P., Plyusnina, A., Berny, P., Cochez, C., Artois, M., Zizi, M., Pirnay, J.P., Plyusnin, A., 2004. Seoul hantavirus in Europe: first demonstration of the virus genome in wild *Rattus norvegicus* captured in France. Eur. J. Clin. Microbiol. Infect. Dis. 23, 711–717.

Hujakka, H., Koistinen, V., Eerikainen, P., Kuronen, I., Laatikainen, A., Kauppinen, J., Vaheri, A., Vapalahti, O., Narvanen, A., 2001a. Comparison of a new immunochromatographic rapid test with a commercial EIA for the detection of Puumala virus specific IgM antibodies. J. Clin. Virol. 23, 79–85.

Hujakka, H., Koistinen, V., Eerikainen, P., Kuronen, I., Mononen, I., Parviainen, M., Lundkvist, A., Vaheri, A., Narvanen, A., Vapalahti, O., 2001b. New immunochromatographic rapid test for diagnosis of acute Puumala virus infection. J. Clin. Microbiol. 39, 2146–2150.

Hujakka, H., Koistinen, V., Kuronen, I., Eerikainen, P., Parviainen, M., Lundkvist, A., Vaheri, A., Vapalahti, O., Narvanen, A., 2003. Diagnostic rapid tests for acute hantavirus infections: specific tests for Hantaan, Dobrava and Puumala viruses versus a hantavirus combination test. J. Virol. Methods 108, 117–122.

Johansson, P., Yap, G., Low, H.T., Siew, C.C., Kek, R., Ng, L.C., Bucht, G., 2010. Molecular characterization of two hantavirus strains from different *Rattus* species in Singapore. Virol. J. 7, 15.

Kariwa, H., Kimura, M., Yoshizumi, S., Arikawa, J., Yoshimatsu, K., Takashima, I., Hashimoto, N., 1996. Modes of Seoul virus infections: persistency in newborn rats and transiency in adult rats. Arch. Virol. 141, 2327–2338.

Kitamura, T., Morita, C., Komatsu, T., Sugiyama, K., Arikawa, J., Shiga, S., Takeda, H., Akao, Y., Imaizumi, K., Oya, A., Hashimoto, N., Urasawa, S., 1983. Isolation of virus causing hemorrhagic-fever with renal syndrome (HFRS) through a cell-culture system. Jpn. J. Med. Sci. Biol. 36, 17–25.

Koma, T., Yoshimatsu, K., Pini, N., Safronetz, D., Taruishi, M., Levis, S., Endo, R., Shimizu, K., Yasuda, S.P., Ebihara, H., Feldmann, H., Enria, D., Arikawa, J., 2010. Truncated hantavirus nucleocapsid proteins for serotyping Sin Nombre, Andes, and Laguna Negra hantavirus infections in humans and rodents. J. Clin. Microbiol. 48, 1635–1642.

Koma, T., Yoshimatsu, K., Yasuda, P.S., Li, T.C., Amada, T., Shimizu, K., Isozumi, R., Mai le, T.Q., Hoa, N.T., Nguen, T., Yamashiro, T., Hasebe, F., Arikawa, J., 2012. A survey of rodent-borne pathogens carried by wild *Rattus* spp. in Northern Vietnam. Epidemiol. Infect., November 1: 1–9. [Epub ahead of print].

Korch, G.W., Childs, J.E., Glass, G.E., Rossi, C.A., Leduc, J.W., 1989. Serologic evidence of hantaviral infections within small mammal communities of Baltimore, Maryland: spatial and temporal patterns and host range. Am. J. Trop. Med. Hyg. 41, 230–240.

Kunita, S., Kato, K., Ishida, M., Hagiwara, K., Kameda, S., Ishida, T., Takakura, A., Goto, K., Sugiyama, F., Yagami, K., 2011. Simultaneous detection of antibodies to mouse hepatitis virus recombinant structural proteins by a microsphere-based multiplex fluorescence immunoassay. Clin. Vaccine Immunol. 18, 758–766.

Lee, H.W., Baek, L.J., Johnson, K.M., 1982. Isolation of Hantaan Virus, the etiologic agent of Korean hemorrhagic-fever, from wild urban rats. J. Infect. Dis. 146, 638–644.

Li, T.C., Yoshimatsu, K., Yasuda, S.P., Arikawa, J., Koma, T., Kataoka, M., Ami, Y., Suzaki, Y., Mai le, T.Q., Hoa, N.T., Yamashiro, T., Hasebe, F., Takeda, N., Wakita, T., 2011. Characterization of self-assembled virus-like particles of rat hepatitis E virus generated by recombinant baculoviruses. J. Gen. Virol. 92, 2830–2837.

Lledo, L., Gegundez, M.I., Saz, J.V., Alves, M.J., Beltran, M., 2002. Serological study of hantavirus in man in the autonomous community of Madrid, Spain. J. Med. Microbiol. 51, 861–865.

Lloyd, G., Bowen, E.T., Jones, N., Pendry, A., 1984. HFRS outbreak associated with laboratory rats in UK. Lancet 1, 1175–1176.

McCaughey, C., Montgomery, W.I., Twomey, N., Addley, M., O'Neill, H.J., Coyle, P.V., 1996. Evidence of hantavirus in wild rodents in Northern Ireland. Epidemiol. Infect. 117, 361–365.

Morii, M., Yoshimatsu, K., Arikawa, J., Zhou, G., Kariwa, H., Takashima, I., 1998. Antigenic characterization of Hantaan and Seoul virus nucleocapsid proteins expressed by recombinant baculovirus: application of a truncated protein, lacking an antigenic region common to the two viruses, as a serotyping antigen. J. Clin. Microbiol. 36, 2514–2521.

Navarrete, M., Barrera, C., Zaror, L., Otth, C., 2007. Rapid immunochromatographic test for hantavirus Andes contrasted with capture-IgM ELISA for detection of andes-specific IgM antibodies. J. Med. Virol. 79, 41–44.

Nemirov, K., Vapalahti, O., Lundkvist, A., Vasilenko, V., Golovljova, I., Plyusnina, A., Niemimaa, J., Laakkonen, J., Henttonen, H., Vaheri, A., Plyusnin, A., 1999. Isolation and characterization of Dobrava hantavirus carried by the striped field mouse (*Apodemus agrarius*) in Estonia. J. Gen. Virol. 80 (Pt 2), 371–379.

Plyusnin, A., Morzunov, S.P., 2001. Virus evolution and genetic diversity of hantaviruses and their rodent hosts. Curr. Top. Microbiol. Immunol. 256, 47–75.

Plyusnin, A., Vapalahti, O., Lundkvist, A., 1996. Hantaviruses: genome structure, expression and evolution. J. Gen. Virol. 77, 2677–2687.

Plyusnina, A., Ibrahim, I.N., Winoto, I., Porter, K.R., Gotama, I.B.I., Lundkvist, A., Vaheri, A., Plyusnin, A., 2004. Identification of Seoul hantavirus in *Rattus norvegicus* in Indonesia. Scand. J. Infect. Dis., 36.

Reynes, J.M., Soares, J.L., Hue, T., Bouloy, M., Sun, S., Kruy, S.L., Flye Sainte Marie, F., Zeller, H., 2003. Evidence of the presence of Seoul virus in Cambodia. Microbes Infect. 5, 769–773.

Schmaljohn, C., Hjelle, B., 1997. Hantaviruses: a global disease problem. Emerg. Infect. Dis. 3, 95–104.

Schmaljohn, C.S., Chu, Y.K., Schmaljohn, A.L., Dalrymple, J.M., 1990. Antigenic subunits of Hantaan virus expressed by baculovirus and vaccinia virus recombinants. J. Virol. 64, 3162–3170.

Seijo, A., Pini, N., Levis, S., Coto, H., Deodato, B., Cernigoi, B., de Bassadoni, D., Enria, D., 2003. Study of hantavirus Seoul in a human and rodent population from a marginal area in Buenos Aires City. Medicina (B Aires) 63, 193–196.

Sirola, H., Kallio, E.R., Koistinen, V., Kuronen, I., Lundkvist, A., Vaheri, A., Vapalahti, O., Henttonen, H., Narvanen, A., 2004. Rapid field test for detection of hantavirus antibodies in rodents. Epidemiol. Infect. 132, 549–553.

Song, G., 1999. Epidemiological progresses of hemorrhagic fever with renal syndrome in China. Chin. Med. J. 112, 472–477.

Truong, T.T., Yoshimatsu, K., Araki, K., Lee, B.H., Nakamura, I., Endo, R., Shimizu, K., Yasuda, S.P., Koma, T., Taruishi, M., Okumura, M., Truong, U.N., Arikawa, J., 2009. Molecular epidemiological and serological studies of hantavirus infection in northern Vietnam. J. Vet. Med. Sci. 71, 1357–1363.

Wang, H., Yoshimatsu, K., Ebihara, H., Ogino, M., Araki, K., Kariwa, H., Wang, Z., Luo, Z., Li, D., Hang, C., Arikawa, J., 2000. Genetic diversity of hantaviruses isolated in china and characterization of novel hantaviruses isolated from *Niviventer confucianus* and *Rattus rattus*. Virology 278, 332–345.

Weissenbacher, M.C., Cura, E., Segura, E.L., Hortal, M., Baek, L.J., Chu, Y.K., Lee, H.W., 1996. Serological evidence of human hantavirus infection in Argentina, Bolivia and Uruguay. Medicina (B Aires) 56, 17–22.

Wu, Y.W., Hsu, E.L., Lin, T.H., Huang, J.H., Chang, S.F., Pai, H.H., 2007. Seaport as a source of hantavirus: a study on isolated isles. Int. J. Environ. Health Res. 17, 25–32.

Yamada, T., Hjelle, B., Lanzi, R., Morris, C., Anderson, B., Jenison, S., 1995. Antibody responses to Four Corners hantavirus infections in the deer mouse (*Peromyscus maniculatus*): identification of an immunodominant region of the viral nucleocapsid protein. J. Virol. 69, 1939–1943.

Yasuda, S.P., Yoshimatsu, K., Koma, T., Shimizu, K., Endo, R., Isozumi, R., Arikawa, J., 2012. Application of truncated nucleocapsid protein (N) for serotyping ELISA of murinae-associated hantavirus infection in rats. J. Vet. Med. Sci. 74, 215–219.

Yoshimatsu, K., Arikawa, J., Kariwa, H., 1993. Application of a recombinant baculovirus expressing hantavirus nucleocapsid protein as a diagnostic antigen in IFA test: cross reactivities among 3 serotypes of hantavirus which causes hemorrhagic fever with renal syndrome (HFRS). J. Vet. Med. Sci. 55, 1047–1050.

Yoshimatsu, K., Arikawa, J., Tamura, M., Yoshida, R., Lundkvist, A., Niklasson, B., Kariwa, H., Azuma, I., 1996. Characterization of the nucleocapsid protein of Hantaan virus strain 76-118 using monoclonal antibodies. J. Gen. Virol. 77, 695–704.

Zhang, Y., Zhang, H., Dong, X., Yuan, J., Zhang, H., Yang, X., Zhou, P., Ge, X., Li, Y., Wang, L.F., Shi, Z., 2010. Hantavirus outbreak associated with laboratory rats in Yunnan, China. Infect. Genet. Evol. 10, 638–644.

JVI
Journals.ASM.org

Involvement of the Rabies Virus Phosphoprotein Gene in Neuroinvasiveness

Satoko Yamaoka,[a] Naoto Ito,[a,b] Seii Ohka,[c] Shohei Kaneda,[d,e] Hiroko Nakamura,[d,e] Takahiro Agari,[b] Tatsunori Masatani,[a]* Keisuke Nakagawa,[a] Kazuma Okada,[a] Kota Okadera,[a] Hiromichi Mitake,[a] Teruo Fujii,[d,e] Makoto Sugiyama[a,b]

The United Graduate School of Veterinary Sciences,[a] and Laboratory of Zoonotic Diseases, Faculty of Applied Biological Sciences,[b] Gifu University, Gifu, Japan; Department of Microbiology, Graduate School of Medicine, Neurovirology Project Department of Genome Medicine, Tokyo Metropolitan Institute of Medical Science, Setagaya-ku, Tokyo, Japan[c]; Institute of Industrial Science, The University of Tokyo, Meguro-ku, Tokyo, Japan[d]; JST CREST, Tokyo, Japan[e]

Rabies virus (RABV), which is transmitted via a bite wound caused by a rabid animal, infects peripheral nerves and then spreads to the central nervous system (CNS) before causing severe neurological symptoms and death in the infected individual. Despite the importance of this ability of the virus to spread from a peripheral site to the CNS (neuroinvasiveness) in the pathogenesis of rabies, little is known about the mechanism underlying the neuroinvasiveness of RABV. In this study, to obtain insights into the mechanism, we conducted comparative analysis of two fixed RABV strains, Nishigahara and the derivative strain Ni-CE, which cause lethal and asymptomatic infections, respectively, in mice after intramuscular inoculation. Examination of a series of chimeric viruses harboring the respective genes from Nishigahara in the genetic background of Ni-CE revealed that the Nishigahara phosphoprotein (P) gene plays a major role in the neuroinvasiveness by mediating infection of peripheral nerves. The results obtained from both *in vivo* and *in vitro* experiments strongly suggested that the Nishigahara P gene, but not the Ni-CE P gene, is important for stable viral replication in muscle cells. Further investigation based on the previous finding that RABV phosphoprotein counteracts the host interferon (IFN) system demonstrated that the Nishigahara P gene, but not the Ni-CE P gene, functions to suppress expression of the beta interferon (IFN-β) gene (*Ifn*-β) and IFN-stimulated genes in muscle cells. In conclusion, we provide the first data strongly suggesting that RABV phosphoprotein assists viral replication in muscle cells by counteracting the host IFN system and, consequently, enhances infection of peripheral nerves.

Rabies virus (RABV), a member of the genus *Lyssavirus* of the family *Rhabdoviridae*, infects almost all kinds of mammals, including humans, and causes a severe neurological disease with a high mortality rate of about 100% after a long and inconstant incubation period (usually 20 to 90 days in humans) (reviewed in reference 1). It is estimated that more than 55,000 people die of rabies every year, mainly in Asia and Africa (2), due to the absence of an effective cure and also the complexity and expensiveness of current postexposure prophylaxis, which requires medical treatment (i.e., rabies vaccination) five times over a period of 28 days. In order to develop both therapeutic and novel prophylaxis approaches for rabies, it is necessary to fully understand the pathogenesis of rabies.

The pathogenesis of rabies essentially relies on viral spread to and in the nervous system of the infected individual (reviewed in reference 1). RABV secreted into saliva of a rabid animal is generally transmitted via a bite wound caused by the infected animal. After transmission, RABV infects peripheral nerves and then spreads to the central nervous system (CNS) via retrograde axonal transport, followed by active viral replication and spread in the CNS, culminating in severe neurological symptoms and lethal outcome. To date, studies on pathogenesis of rabies have mainly focused on ability of the virus to spread in the CNS and to cause disease (neurovirulence), and results of those studies have revealed that the cell-to-cell infection and viral evasion of neuronal apoptosis and innate immunity contribute to the neurovirulence of RABV (3–6).

In contrast, less is known about ability of the virus to spread from a peripheral site to the CNS (neuroinvasiveness). For instance, it is not clear whether RABV replication in nonneural peripheral tissue is an important key to infection of peripheral nerves. Previous histopathological studies using animals inoculated with street RABV strains (field isolates) or fixed RABV strains (laboratory and vaccine strains) via the intramuscular (i.m.) route have demonstrated the presence of the viral antigen in muscle cells prior to detection of the antigen in peripheral nerves (7–10). These observations indicate the possibility that RABV replication in muscle cells contributes to efficient infection of peripheral nerves. However, this possibility has been questioned by results of other previous studies using both street and fixed RABV strains, strongly suggesting that RABV directly infects peripheral nerves without replication in muscle cells after i.m. inoculation (11–13). Therefore, the contribution of RABV replication in muscle cells to infection of peripheral nerves is still controversial. This is mainly due to a lack of experimental data showing a strong relationship between viral replication in muscle cells and infection of peripheral nerves.

The RABV particle contains an unsegmented negative-sense genomic RNA encoding five structural proteins: nucleoprotein (N), phosphoprotein (P), matrix (M) protein, glycoprotein (G), and large (L) protein (reviewed in reference 14). The N, P, and L

Received 1 August 2013 **Accepted** 2 September 2013
Published ahead of print 11 September 2013
Address correspondence to Makoto Sugiyama, sugiyama@gifu-u.ac.jp.
* Present address: Tatsunori Masatani, National Research Center for Protozoan Diseases, Obihiro University of Agriculture and Veterinary Medicine, Inada-cho, Obihiro, Hokkaido, Japan.

doi:10.1128/JVI.02132-13

proteins and viral genomic RNA constitute a ribonucleoprotein (RNP) complex. The N protein enwraps the genomic RNA, whereas the P protein, in combination with the L protein, known as an RNA-dependent RNA polymerase, is involved in viral RNA synthesis. The P protein also functions as an interferon (IFN) antagonist by inhibiting both IFN induction and response (4, 15–21). The M protein, which interacts with both the RNP and G protein, participates in recruiting RNP to the host cell membrane and budding of enveloped virus particles. The G protein forms spikes that project from the viral envelop and plays an indispensable role in interaction with receptors on host cells.

Among these viral proteins, G protein is known to play an important role in the neuroinvasiveness of RABV. Prehaud et al. (22) demonstrated by i.m. inoculation of mice with a series of neutralizing escape mutants that Lys-to-Gln mutation at position 147 in G protein significantly decreases the lethality of an RABV strain. Notably, it was shown that lentiviral vectors pseudotyped with RABV G protein invade peripheral nerves and reach the CNS after i.m. inoculation (23, 24), clearly indicating that G protein is responsible for both internalization to peripheral nerves and retrograde axonal transport of RABV. Other previous studies also indicated or strongly suggested the importance of G protein in the neuroinvasiveness of RABV (25–29).

Meanwhile, there is also accumulating evidence that viral proteins other than G protein are also involved in the neuroinvasiveness of RABV. Pulmanausahakul et al. (27) showed by comparative analysis of the highly neuroinvasive SB strain and attenuated SN strain that, after i.m. inoculation, the chimeric virus with the G gene from the SB strain in the genetic background of the SN strain causes lower morbidity and mortality in mice than does the SB strain. This indicates that viral proteins other than G protein also contribute to the ability of the SB strain to infect peripheral nerves, to invade the CNS, and to cause lethal neurological symptoms. Indeed, further analysis and a previous study revealed that the M and L genes play supplementary roles in these abilities of SB strain (25, 27). However, the roles of RABV proteins other than G protein in the neuroinvasiveness still remain to be elucidated.

We previously reported that the fixed RABV strain Nishigahara (Ni) causes lethal neurological symptoms in mice after intracerebral (i.c.) inoculation, whereas the derivative Ni-CE strain causes mild symptoms, such as transient body weight loss in mice (30). Although these strains differ in lethality in mice, this indicates that both strains have the ability to infect neurons in the brain and to cause symptomatic infection in mice. Interestingly, we found that, after i.m. inoculation, the Ni-CE strain causes asymptomatic infection in mice, in contrast to the Ni strain, which causes lethal symptomatic infection (unpublished data). Therefore, the Ni and Ni-CE strains differ in neuroinvasiveness in mice.

In the present study, we examined the mechanisms underlying the different levels of neuroinvasiveness of the Ni and Ni-CE strains by analyzing a series of chimeric viruses with the respective genes from Ni strain in the genetic background of the Ni-CE strain. The results indicated that the P gene is mainly responsible for the different levels of neuroinvasiveness of the Ni and Ni-CE strains and mediates their abilities to infect peripheral nerves. We also demonstrated that the Ni P gene, but not the Ni-CE P gene, functions to assist viral replication in muscle cells. The findings obtained from further experiments based on the IFN-antagonistic function of RABV P protein (4, 15–21) revealed that the Ni P gene, but not the Ni-CE P gene, functions to evade induction of the IFN-β (*Ifn*-β) gene and IFN-stimulated genes (ISGs), such as the myxovirus resistance A (*Mx1*) and 2′-5′-oligoadenylate synthetase 1 (*Oas1*) genes. This study provides the first data strongly suggesting that replication of RABV in muscle cells, which is supported by the P protein's IFN-antagonistic function, enhances infection of peripheral nerves.

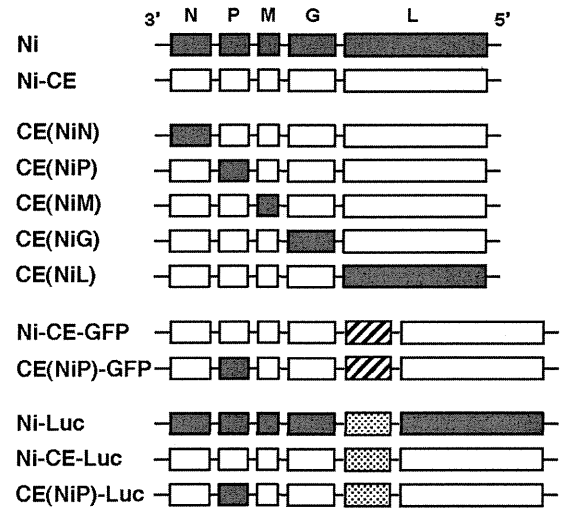

FIG 1 Schematic diagrams of genome organizations of the RABV strains used in this study. The black and white bars represent the viral genes that originate from Ni and Ni-CE strains, respectively. The striped bars and dotted bars represent the GFP gene and the firefly luciferase gene, respectively.

MATERIALS AND METHODS

Cells. Mouse neuroblastoma NA cells were maintained in Eagle's minimal essential medium (EMEM) supplemented with 10% fetal calf serum (FCS). Mouse muscle myoblast G-8 cells (American Type Culture Collection [ATCC] no. CRL-1456) were grown in high-glucose Dulbecco's modified Eagle's medium (DMEM) supplemented with 10% FCS and 10% horse serum (HS). Mouse muscle myoblast C2C12 cells (ATCC no. CRL-1772) and human rhabdomyosarcoma A-673 cells (ATCC no. CRL-1598) were grown in DMEM supplemented with 10% FCS. Differentiation of G-8 and C2C12 cells was carried out according to the instructions of ATCC. Briefly, G-8 and C2C12 cells were differentiated by reducing the FCS and HS to 2% each and by supplying 10% HS instead of FCS to the growth medium, respectively.

Viruses. As Ni and Ni-CE strains, we used recombinant viruses of the respective strains that had been recovered from cloned cDNA (30, 31). Chimeric CE(NiN), CE(NiP), CE(NiM), CE(NiG), and CE(NiL) strains with respective genes of the Ni strain in the background of the Ni-CE genome were also previously generated by a reverse-genetics approach (30) (Fig. 1).

To generate a recombinant Ni-CE strain expressing green fluorescent protein (GFP) (Ni-CE-GFP) (Fig. 1), we amplified a cDNA fragment containing the GFP gene downstream of transcriptional stop and start signals of RABV by PCR using the pEGFP-N1 vector (Clontech, Mountain View, CA) as a template and then inserted the fragment into the G-L intergenic region (upstream of the transcriptional stop signal of the G gene) of the full-length genome plasmid of the Ni-CE strain. We rescued the Ni-CE-GFP strain from the resulting plasmid, as previously reported (32). In the same manner, we generated a recombinant chimeric CE(NiP) strain expressing GFP [CE(NiP)-GFP] from the full-length genome plasmid. Recombinant Ni, Ni-CE, and chimeric CE(NiP) strains expressing firefly luciferase [Ni-Luc, Ni-CE-Luc, and CE(NiP)-Luc, respectively] (Fig. 1) were generated by the same procedure as that described above using pGL3-Control vector (Promega, Madison, WI) as a template for PCR.

TABLE 1 Sequences of the primers used in this study

Analysis	Primer (sense)	Sequence (5′ to 3′)	Annealing site positions[a]
RT	RHN19 (+)	AAAATGTAACACCTCTACAATG	52–73
PCR			
1st	N501 (+)	TCCTGAGTCTGTATAGGTTGAGCAA	501–525
	RHN18 (−)	CCATGTAGCATCCAACAAAGT	1008–1028
2nd	N540 (+)	ACACCGGTAACTATAAAACAAACAT	540–564
	N1000 (−)	ATTGAACACATGACCAACGGCATTC	976–1000

[a] Site from the 5′-terminal region of the full-genome sequence of the RABV Ni strain (accession no. AB044824.1).

Details of the construction of these plasmids and sequences of the primers are available from the authors on request. All virus stocks were prepared in NA cells and stored at −80°C. Titers of viruses were determined by focus assays in NA cells using monoclonal antibody 13-27 against RABV N protein (33) and fluorescein isothiocyanate (FITC)-labeled goat IgG anti-mouse IgG.

Pathogenicity of each virus in mice. Five 4-week-old female ddY mice (Japan SLC, Inc., Shizuoka, Japan) per group were inoculated intracerebrally with 0.03 ml of 10^6 focus-forming units (FFU) of each strain or intramuscularly with 0.1 ml of 10^6 FFU of each strain into the left thigh muscle. In another experiment, 20 mice per group were intramuscularly inoculated with 10^6 FFU of the Ni-CE or CE(NiP) strain. The mice were observed daily for 14 days. The symptoms in mice were classified into 5 grades: (i) normal, (ii) body weight loss (5% reduction from maximum body weight), (iii) mild neurological symptoms (such as stagger or gait abnormality of a unilateral hind limb), (iv) severe neurological symptoms (such as gait abnormality of bilateral hind limbs), and (v) death. We euthanized mice when they showed lack of righting reflex (mice unable to right themselves within 10 s after being placed on their side). All animal experiments in this study were conducted in accordance with the Regulations for Animal Experiments in Gifu University; the protocols were approved by the Committee for Animal Research and Welfare of Gifu University (approval no. 10086).

Biodistribution of each strain in mice. Three 4-week-old ddY mice (Japan SLC, Inc.) per group were intramuscularly inoculated with 10^6 FFU of the Ni or Ni-CE strain, and five mice per group were inoculated with the CE(NiP) strain. Mice were euthanized at 5 days postinoculation (dpi), and their brains, spinal cords at cervical spine 1 (C1) to the last lumbar vertebra, sciatic nerves, and thigh muscles were quickly collected. In another experiment, 10 mice per group were intramuscularly inoculated with 10^6 FFU of the Ni-CE or CE(NiP) strain, and their sciatic nerves and thigh muscles were collected at 8 dpi. Tissues were frozen in liquid nitrogen and stored at −80°C until being used for RNA extraction and reverse transcription (RT)-nested PCR. After the stored tissues were thawed and homogenized, total RNAs were extracted from each tissue using TRIzol reagent (Invitrogen, Carlsbad, CA) and were purified using a PureLink RNA minikit (Invitrogen) according to the manufacturer's instructions. The extracted RNAs were reverse transcribed into cDNAs by using SuperScript III reverse transcriptase (Invitrogen) with reverse transcriptase primer RHN19(+) specific to the RABV genome (Table 1). First and 2nd PCRs were performed with TaKaRa HS *Ex Taq* (TaKaRa Bio, Inc., Shiga, Japan) using primer pairs N501(+)-RHN18(−) and N540(+)-N1000(−), respectively, which are specific to the N gene regions of the RABV genome (Table 1).

***In vitro* examination of the ability of the virus to infect neurons via axon terminals.** Microfluidic culture platforms with two compartments connected by 450-μm-long microgrooves, which allow cell bodies of primary cultured neurons and their axon terminals to grow separately, were fabricated in polydimethylsiloxane (PDMS) based on previous studies (34), and protocols for assembly of the culture platform and dish were modified from previous reports (34, 35). In brief, a culture platform was placed on a lumox dish (Sarstadt, Numbrecht, Germany), and the culture platform and dish were coated with 1,500 μg/ml of poly-DL-ornithine (Sigma-Aldrich, Saint Louis, MO) for 2 days at 4°C. On the day of cell plating, after being washed with phosphate-buffered saline (PBS), the culture platform and dish were coated with 3 μg/ml laminin (Sigma) for 5 h at 37°C.

Primary cultured motor neurons were prepared as described previously (36). Briefly, spinal cords were dissected from embryos of ICR mice (Japan SLC, Inc.) at embryonic day 13 and incubated at 37°C in 0.025% trypsin (Invitrogen) for 10 min. Tissue was resuspended in neurobasal medium (Invitrogen) containing bovine serum albumin (Sigma) and DNase I (Sigma). After dissociation of tissue by gently pipetting, the supernatant containing cells was collected and centrifuged at 340 × *g* for 5 min. The cell pellet was resuspended in the enriched medium (37), and cells were plated in the cell body side of the coated culture platform at densities of approximately 4×10^6 cells/ml. The culture medium was replaced at 3 days postplating, and cultures were kept in a CO_2-regulated 37°C incubator.

At 5 days postplating, after axons had extended across the microgrooves, cells were infected with the Ni-CE-GFP or CE(NiP)-GFP strain from the axon terminal side of the culture platform. Briefly, the wells of the axon terminal side were completely depleted of medium, and they were inoculated with 10^6 FFU of each virus. After a 1-h incubation for virus adsorption, the virus inoculum in wells of the axon terminal side was removed and replaced with enriched medium. The medium in wells of the axon terminal side was maintained at a lower volume than that of medium in wells of the cell body side. This hydrostatic pressure completely prevented diffusion of virus through the microgrooves to the cell body side of the culture platform. At 12, 24, 36, and 48 h postinoculation (hpi), cell bodies were observed by using a Biozero fluorescence microscope (BZ-8000 series; Keyence, Osaka, Japan), and then the percentages of GFP-positive cell bodies were calculated. Images were analyzed by using IMARIS (Carl Zeiss Microscopy Co., Ltd., Oberkochen, Germany).

***In vivo* examination of viral replication in muscle.** Three 4-week-old ddY mice (Japan SLC, Inc.) per group were intramuscularly inoculated with 10^6 FFU of the Ni-Luc, Ni-CE-Luc, or CE(NiP)-Luc strain. Thigh muscles of infected mice were collected at 0, 12, 24, and 72 hpi, and then they were homogenized and lysed by using 1 ml of passive lysis buffer (Promega), and the samples were stored at −80°C. After being thawed and vortexed, the samples were centrifuged at 20,600 × *g* for 5 min, and then 10 μl of each of the supernatants was used to measure luciferase activities (calculated as relative light units [RLU]/s/g muscle weight) with the Promega luciferase assay systems.

***In vitro* examination of viral replication in muscle cell lines.** Differentiated G-8, C2C12, and A-673 cells grown in a 24-well tissue culture plate were infected with the Ni-Luc, Ni-CE-Luc, or CE(NiP)-Luc strain at a multiplicity of infection (MOI) of 1. The cells were lysed at 7 dpi by using 100 μl of Promega cell culture lysis reagent and stored at −80°C until use. After being thawed and vortexed, the samples were centrifuged at 13,200 × *g* for 2 min, and then 10 μl of each of the supernatants was used for the luciferase assays as described above.

Differentiated G-8 cells grown in a 6-well tissue culture plate were infected with the Ni, Ni-CE, or CE(NiP) strain at an MOI of 1. At 1, 3, 5, and 7 dpi, viruses in the culture supernatants were harvested and titrated in NA cells by focus assays, as described above. All assays were carried out in triplicate, and the results are expressed as means ± standard errors of the means.

Real-time RT-PCR. Differentiated G-8 cells grown in a 24-well tissue culture plate were infected with the Ni, Ni-CE, or CE(NiP) strain at an MOI of 1. At 24 hpi, total RNAs were extracted using an RNeasy Plus minikit (Qiagen, Hilden, Germany) and reverse transcribed into cDNAs with a random primer [hexadeoxyribonucleotide mixture; pd $(N)_6$] (TaKaRa Bio). The expression of the *Ifn*-β, *Mx1*, *Oas1*, and *Gapdh* (glyceraldehyde-3-phosphate dehydrogenase) genes in the infected cells was analyzed by using a TaqMan gene expression master mix (Applied Biosystems, Carls-

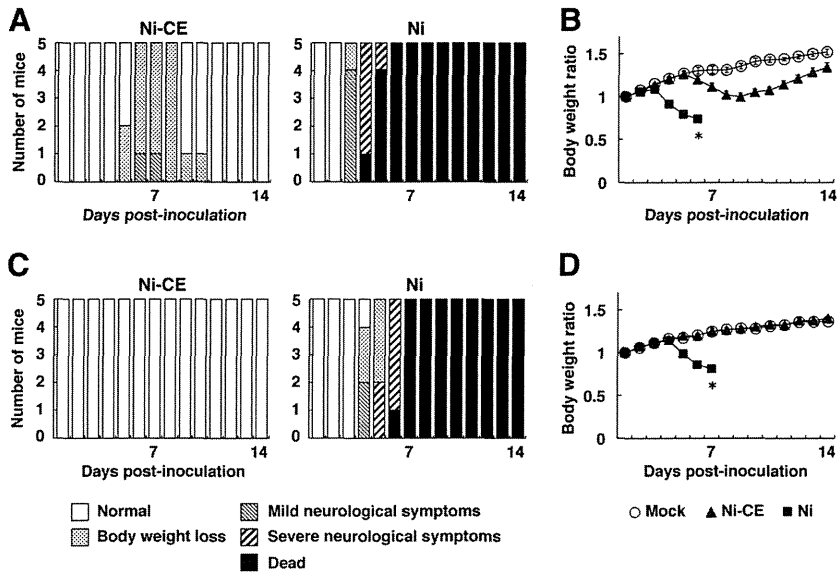

FIG 2 Progression of symptoms and changes in body weight of mice inoculated (A and B) intracerebrally or (C and D) intramuscularly with 10^6 FFU of the Ni or Ni-CE strain. The mice were observed daily for 14 days. The symptoms in mice were classified into 5 grades: (i) normal, (ii) body weight loss, (iii) mild neurological symptoms, (iv) severe neurological symptoms, and (v) death. The changes in body weight are shown as ratios, considering the body weights of mice at day 0 as 1. The values in the graph are averages and standard errors of the ratio. *, all of the mice died.

bad, CA) with specific TaqMan probes (Ifn-β [Mm00439546], Mx1 [Mm00487796], Oas1 [Mm00449297], and GAPDH [4352339E]) in an ABI 7300 real-time PCR system (Applied Biosystems). The expression levels of *Ifn-β*, *Mx1*, and *Oas1* genes are indicated as the number of copies of specific mRNA per copy of mouse *Gapdh* mRNA. All assays were carried out in triplicate, and the values in the graph are shown as means ± standard errors of the means.

In another experiment, three 4-week-old ddY mice (Japan SLC, Inc.) per group were intramuscularly inoculated with 10^6 FFU of the Ni, Ni-CE, or CE(NiP) strain. Thigh muscles of infected mice were collected at 12 hpi, and then total RNAs were extracted from each tissue using TRIzol reagent (Invitrogen) and a PureLink RNA minikit (Invitrogen). The extracted RNAs were reverse transcribed into cDNAs, and the expression of the *Ifn-β* and *Gapdh* genes in the thigh muscles of infected mice was analyzed by the same method described above. The values in the graph are shown as means ± standard errors of the means.

Statistical analysis. Student's *t* test was used to determine statistical significance. *P* values of <0.05 were considered statistically significant.

RESULTS

Examination of pathogenicities of Ni and Ni-CE strains in mice by i.c. and i.m. inoculations. To confirm the different levels of neuroinvasiveness of the Ni and Ni-CE strains, we examined their pathogenicities in 4-week-old mice by both i.c. and i.m. inoculations (Fig. 2). After i.c. inoculation, all of the mice infected with the Ni and Ni-CE strains developed symptoms, although the severities of infection were clearly different: all of the Ni-infected mice died within 6 dpi after showing obvious neurological symptoms, whereas all of the Ni-CE-infected mice survived following transient body weight loss and, occasionally, mild neurological symptoms (Fig. 2A and B). These results strongly suggest that both the Ni and Ni-CE strains have the ability to cause symptomatic infection in mice once they have reached the brain. After i.m. inoculation, all of the Ni-infected mice developed severe neurological symptoms, similar to those after i.c. inoculation, and died within 7 dpi. In contrast, all of the Ni-CE-infected mice continuously gained body weight without showing any symptoms (Fig. 2C and D). These findings confirm that the ability of Ni strain to cause symptomatic infection in mice after i.m. inoculation is significantly higher than that of the Ni-CE strain.

Identification of the viral gene related to neuroinvasiveness. To identify the viral gene or genes related to the difference in levels of neuroinvasiveness of the Ni and Ni-CE strains, we examined pathogenicities of chimeric CE(NiN), CE(NiP), CE(NiM), CE(NiG), and CE(NiL) strains, which have N, P, M, G, and L genes from the Ni strain in the genetic background of the Ni-CE strain, respectively (Fig. 1), by i.m. inoculation into 4-week-old mice (Fig. 3). The CE(NiM) and CE(NiL) strains caused asymptomatic infection in mice, as did the Ni-CE strain (Fig. 2C). In contrast, the CE(NiN), CE(NiP), and CE(NiG) strains caused symptomatic infection in some of the mice. We found that 80% of the CE(NiP)-infected mice developed neurological symptoms and died within 13 dpi and that 40% of the CE(NiN)- and CE(NiG)-infected mice showed symptoms and died, except for one mouse that recovered from CE(NiG) infection. These results indicate that multiple viral genes, especially the P gene, are related to the difference in levels of neuroinvasiveness of the Ni and Ni-CE strains. The importance of the Ni P gene in neuroinvasiveness was confirmed by data obtained from two independent experiments showing 75% to 80% morbidity rates of CE(NiP)-infected mice (Table 2). Based on the results, it is concluded that the P gene plays a major role in the ability of the Ni strain to cause symptomatic infection in mice after i.m. inoculation.

Biodistribution of the Ni, Ni-CE, and CE(NiP) strains in mice after i.m. inoculation. To obtain an insight into the mechanism by which the Ni and Ni-CE P genes are differently involved in neuroinvasiveness, we investigated the biodistribution of the Ni, Ni-CE, and CE(NiP) strains in mice after i.m. inoculation. For this purpose, we collected brains, spinal cords, sciatic nerves, and thigh muscles from mice infected with the respective strains at 5

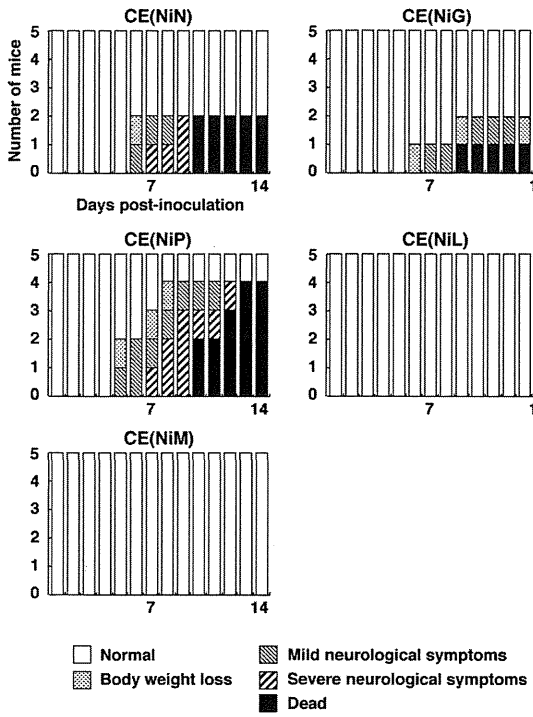

FIG 3 Progression of symptoms in mice inoculated intramuscularly with 10^6 FFU of chimeric strains with the respective genes of the Ni strain in the background of the Ni-CE genome. The mice were observed daily for 14 days.

dpi, when 100% (3/3 mice), 0% (0/3 mice), and 20% (1/5 mice) of Ni-, Ni-CE-, and CE(NiP)-infected mice, respectively, showed symptoms (Fig. 4A). Next, we examined the presence of viral genomic RNAs in these tissues by RT-nested PCR, of which the detection limit is equivalent to 10 FFU of infectious viruses (data not shown). As this RT-nested PCR system is designed to target viral genomic RNAs, the system detects, in addition to viral RNAs of replicating viruses, those of nonreplicating viruses, such as viruses traveling along axons of the sciatic nerve. In all of the infected mice, viral RNAs were detected in thigh muscles, which were the sites of viral inoculation (Fig. 4A). Considering the design and high sensitivity of this RT-nested PCR, it is highly possible that not only genomic RNAs of replicating viruses but also those of nonreplicating viruses contained in the inoculum were detected in muscles. We found that in all of the Ni-infected mice, viral RNAs were present in the brains, spinal cords, and sciatic nerves, whereas in all of the Ni-CE-infected mice, viral RNAs were detected in none of these nerve tissues. In 40% (2/5 mice) of the CE(NiP)-infected mice, viral RNAs were found in all of the examined nerve tissues. These results indicate that the abilities of the Ni and CE(NiP) strains to infect peripheral nerves are higher than that of Ni-CE strain.

To confirm the difference between the abilities of Ni-CE and CE(NiP) strains to infect peripheral nerves, we intramuscularly inoculated 10 mice per group with the Ni-CE or CE(NiP) strain and examined the presence of viral RNA in sciatic nerves and thigh muscles by using the same method at 8 dpi, when 0% (0/10 mice) and 40% (4/10 mice) of Ni-CE- and CE(NiP)-infected mice, respectively, showed symptoms (Fig. 4B). We detected viral RNAs in the thigh muscles of all of the infected mice. Importantly, in 60% (6/10 mice) of the CE(NiP)-infected mice, viral RNAs were found in sciatic nerves, whereas viral RNAs were not detected in sciatic nerves of any of the Ni-CE-infected mice, These results indicate that the Ni P gene, but not the Ni-CE P gene, mediates infection of peripheral nerves.

Abilities of Ni-CE and CE(NiP) strains to infect peripheral nerves. Next, using an *in vitro* system, we examined whether the Ni-CE strain, but not the CE(NiP) strain, has a defect in the ability to infect peripheral nerves via axon terminals. For this purpose, we utilized primary cultured neurons grown by using a microfluidic culture platform, which enables maintenance of their cell body and axon terminal compartments fluidically isolated from each other (Fig. 5A and B). We inoculated the GFP-expressing Ni-CE or CE(NiP) strain [Ni-CE-GFP or CE(NiP)-GFP] (Fig. 1) into the axon terminal side and then checked for the presence of GFP signals in the cell bodies. At 48 hpi, GFP signals were observed in the cell bodies of neurons infected with the Ni-CE-GFP strain and those infected with the CE(NiP)-GFP strain (Fig. 5C). After GFP signals were first detected at 24 hpi, the percentages of GFP-positive cell bodies in both neurons infected with Ni-CE-GFP and CE(NiP)-GFP strains similarly increased over time (Fig. 5D). We confirmed the reproducibility of these results by a repeated experiment (data not shown). These results suggest that both strains invade neurons via axon terminals, travel retrogradely in axons, and replicate in cell bodies with similar efficiencies. Therefore, we concluded that the Ni-CE strain has the ability to infect peripheral nerves via axon terminals.

Contribution of the P gene to viral replication in muscle cells. The above results obtained from *in vitro* experiments are inconsistent with the finding that the Ni-CE strain does not infect peripheral nerves *in vivo* (Fig. 4), leading to the possibility that the Ni and Ni-CE P genes are differently involved in viral replication in muscle. To examine this possibility, we inoculated the firefly luciferase-expressing Ni, Ni-CE, or CE(NiP) strain [Ni-Luc, Ni-CE-Luc, or CE(NiP)-Luc] (Fig. 1) into thigh muscles of mice and compared the activities of luciferase expressed in the inoculated thigh muscles after sequential collections of muscle samples (Fig. 6A). In Ni-Luc- and CE(NiP)-Luc-infected mice, but not in Ni-CE-Luc-infected mice, the luciferase activities in muscle gradually increased over time. At 72 hpi, the luciferase activity in muscle from Ni-Luc-infected mice was significantly higher than that in muscle from Ni-CE-Luc-infected mice ($P < 0.05$). The luciferase activity in muscle from CE(NiP)-Luc-infected mice also tended to be higher than that in muscle from Ni-CE-Luc-infected mice. Viral genomic RNAs were detected in the inoculated thigh mus-

TABLE 2 Morbidity rates of mice inoculated i.m. with each strain

Strain	% morbidity (no. sick/inoculated) in:		
	Expt 1[a]	Expt 2[a]	Expt 3[b]
Ni	100 (5/5)	100 (5/5)	NT[c]
Ni-CE	0 (0/5)	0 (0/5)	0 (0/20)
CE(NiN)	40 (2/5)	20 (1/5)	NT
CE(NiP)	80 (4/5)	80 (4/5)	75 (15/20)
CE(NiM)	0 (0/5)	0 (0/5)	NT
CE(NiG)	40 (2/5)	0 (0/5)	NT
CE(NiL)	0 (0/5)	0 (0/5)	NT

[a] Groups of five mice were i.m. inoculated with each strain.
[b] Groups of 20 mice were i.m. inoculated with the Ni-CE or CE(NiP) strain.
[c] NT, not tested.

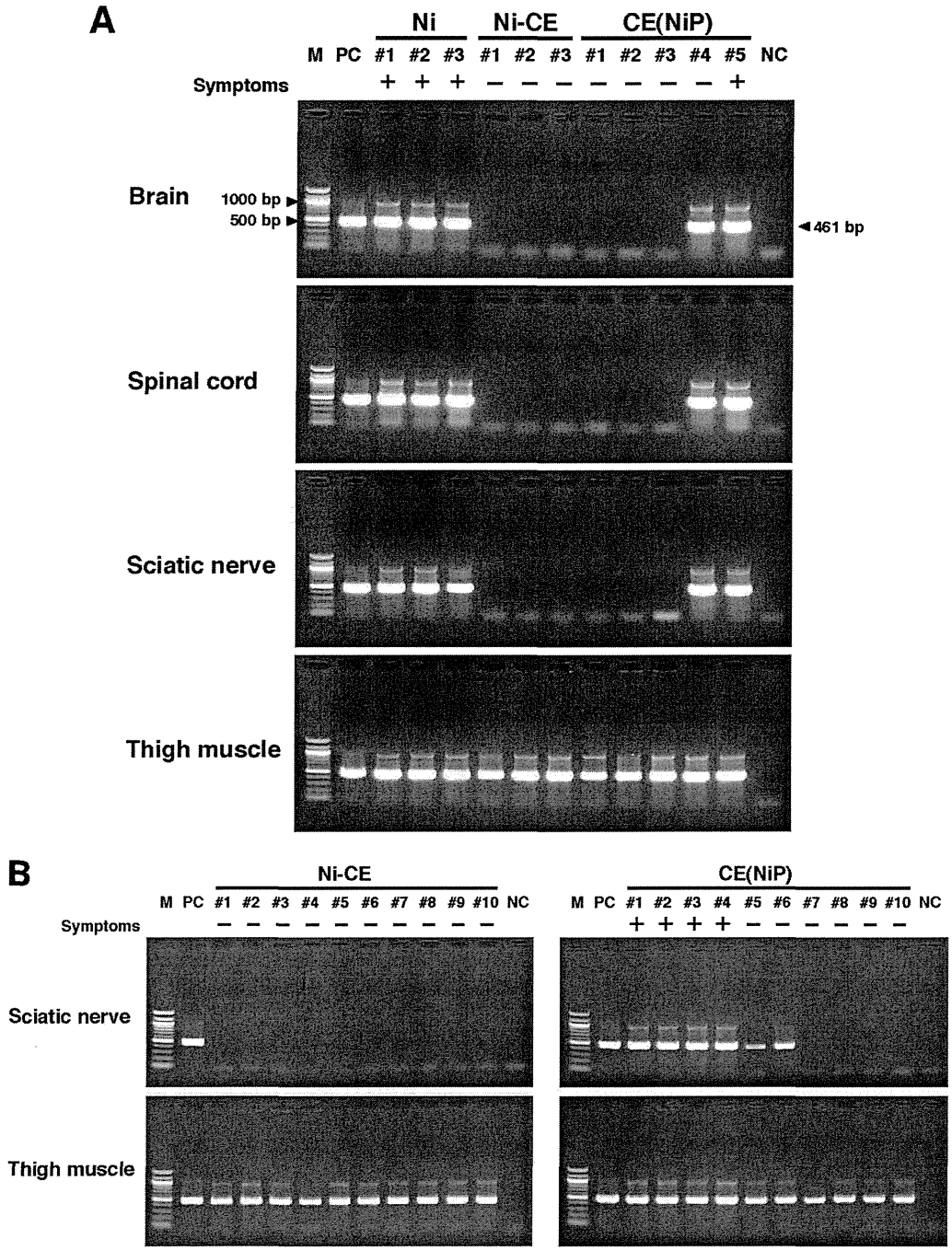

FIG 4 Viral biodistribution in mice inoculated with each strain. Mice were intramuscularly inoculated with 10^6 FFU of the Ni, Ni-CE, or CE(NiP) strain. Tissues were collected (A) at 5 dpi or (B) at 8 dpi and analyzed for viral genomic RNAs by RT-nested PCR targeting the N gene region (461 bp). M, marker; #1 to #10, identification numbers of mice; PC, positive control (mouse brain intracerebrally inoculated with challenge virus standard [CVS] strain); NC, negative control (each tissue i.m. inoculated with medium). Symptoms: +, mouse with symptoms such as body weight loss and neurological symptoms on the day of tissue collection; −, mouse without any symptoms on the day of tissue collection.

cles of all of the infected mice (Fig. 6B), confirming that each strain had been inoculated into thigh muscle. These results suggest that the Ni P gene functions to assist viral replication in muscle *in vivo*.

To investigate the importance of the Ni P gene in viral replication in muscle cells *in vitro*, we inoculated the Ni-Luc, Ni-CE-Luc, or CE(NiP)-Luc strain into three cell lines derived from mouse or human muscle cells and compared the luciferase activities expressed in the infected muscle cells (Fig. 7). We found that the activities in mouse muscle myoblast G-8 cells infected with the Ni-Luc and CE(NiP)-Luc strains were significantly higher than that in cells infected with Ni-CE-Luc strain ($P < 0.05$) (Fig. 7A). Similar results were obtained with infection of mouse muscle myoblast C2C12 cells and human rhabdomyosarcoma A-673 cells

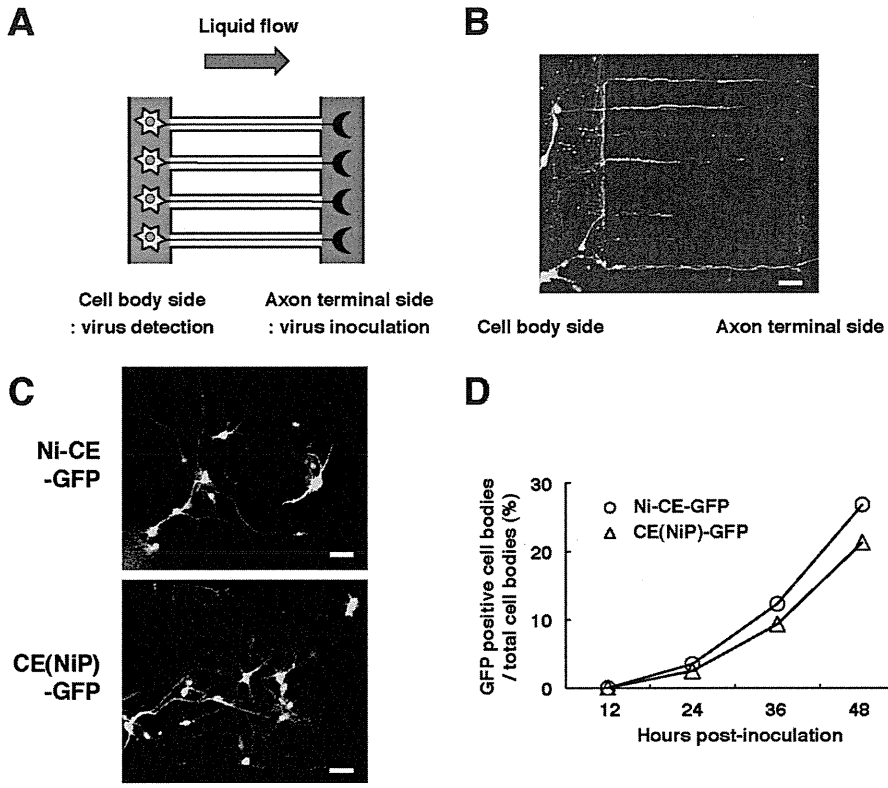

FIG 5 Ability of virus to infect neurons via axon terminals. (A) Diagram of microfluidic culture platform. (B) Image of Ni-CE-GFP-infected neurons at 48 hpi. (C) Cell bodies of Ni-CE-GFP- or CE(NiP)-GFP-infected neurons at 48 hpi. (D) Percentages of GFP-positive cell bodies in neurons infected with the Ni-CE-GFP or CE(NiP)-GFP strain. The scale bars correspond to 50 μm.

with these luciferase-expressing strains (Fig. 7B and C). These results indicate that the efficiencies of replication of the Ni and CE(NiP) strains in these muscle cells are higher than that of the Ni-CE strain.

Next, we compared the levels of production of infectious viruses in G-8 cells infected with the Ni, Ni-CE, and CE(NiP) strains (Fig. 8). The virus titers of the Ni and CE(NiP) strains in culture supernatants slightly increased over time, whereas the titer of the Ni-CE strain drastically decreased: while the titers at 7 dpi of the Ni and CE(NiP) strains reached about 10^5 FFU/ml, the titer of the Ni-CE strain decreased to $<10^2$ FFU/ml ($P < 0.05$). We confirmed that $<10^2$ FFU/ml of the respective viruses was carried over from the inoculum into the culture supernatants at 0 dpi (data not shown). The results presented above indicate that infectious viruses were produced more efficiently in G-8 cells infected with the Ni and CE(NiP) strains than in the cells infected with the Ni-CE strain.

Based on the above findings, it is concluded that the Ni P gene, but not the Ni-CE P gene, mediates stable viral replication in muscle cells, supporting the possibility that viral replication in muscle cells enhances infection of peripheral nerves.

IFN induction and responses in muscle cells infected with the respective strains. According to the results of previous studies showing that RABV P protein functions to antagonize the host IFN system (4, 15–21), we checked whether the CE(NiP) and Ni-CE strains differ in the ability to suppress IFN induction in muscle cells. Specifically, we compared the expression levels of the *Ifn*-β gene and also the *Mx1* and *Oas1* genes, known as ISGs, in G-8 cells infected with the Ni, Ni-CE, and CE(NiP) strains (Fig. 9). To minimize the influence of different replication efficiencies of those strains in G-8 cells, we chose 1 dpi, at which time the titers of the respective strains in the culture supernatants were comparable (Fig. 8), as the time for RNA collection. We found that the expression levels of the *Ifn*-β gene in Ni- and CE(NiP)-infected cells were significantly lower than the level in Ni-CE-infected cells ($P < 0.05$) (Fig. 9A). Similar results were obtained with an equivalent assay using mouse muscle C2C12 cells (data not shown). Consistent with these results, the expression levels of the *Mx1* and *Oas1* genes were suppressed in Ni- and CE(NiP)-infected G-8 cells more efficiently than that in Ni-CE-infected cells ($P < 0.05$) (Fig. 9B and C). These results indicate that the Ni and CE(NiP) strains suppress expression of the *Ifn*-β gene and ISGs in muscle cells more efficiently than does the Ni-CE strain.

To investigate the abilities of the Ni, Ni-CE, and CE(NiP) strains to suppress IFN induction in muscle *in vivo*, we compared the expression levels of the *Ifn*-β gene in inoculated thigh muscles of Ni-, Ni-CE-, and CE(NiP)-infected mice (Fig. 10). We found that expression levels of the *Ifn*-β gene in the muscles from Ni- and CE(NiP)-infected mice tended to be lower than that in the muscles from Ni-CE-infected mice.

These results indicate that the Ni P gene, but not the Ni-CE P gene, functions to suppress IFN induction in muscle cells and also strongly suggest that the function of P protein to antagonize the host IFN system affects the efficiency of viral replication in infected muscle cells.